



Plastic energy allocation toward life-history functions in a consumer-resource interaction

Analyzing the temporal patterns of the consumer-resource dynamics

R. Gutiérrez¹ · F. Córdova-Lepe¹ · F. N. Moreno-Gómez² · N. A. Velásquez³

Received: 29 June 2021 / Revised: 3 November 2022 / Accepted: 7 November 2022 /

Published online: 23 November 2022

© The Author(s), under exclusive licence to Springer-Verlag GmbH Germany, part of Springer Nature 2022

Abstract

Various environmental alterations resulting from the current global change compromise the persistence of species in their habitual environment. To cope with the obvious risk of extinction, plastic responses provide organisms with rapid acclimatization to new environments. The premise of plastic rescue has been theoretically studied from mathematical models in both deterministic and stochastic environments, focusing on analyzing the persistence and stability of the populations. Here, we evaluate this premise in the framework of a consumer-resource interaction considering the energy investment towards reproduction vs. maintenance as a plastic trait according to positive/negative variation of the available resource. A basic consumer-resource mathematical model is formulated based on the principle of biomass conversion that incorporates the energy allocation toward vital functions of the life-cycle of consumer individuals. Our mathematical approach is based on the impulsive differential equations at fixed moments considering two impulsive effects associated with the instants at which consumers obtain environmental information and when energy allocation strategy change occurs. From a preliminary analysis of the non-plastic temporal dynamics, namely when the energy allocation is constant over time and without experiencing changes concerning the variation of resources, both the persistence and stability of the consumer-resource dynamic are dependent on the energy allocation strategies belonging to a set termed stability range. We found that the plastic energy allocation

✉ R. Gutiérrez
rgutierrez@ucm.cl

¹ Departamento de Matemática, Física y Estadística, Facultad de Ciencias Básicas, Universidad Católica del Maule, Talca, Chile

² Laboratorio de Bioacústica y Ecología del Comportamiento Animal, Departamento de Biología y Química, Facultad de Ciencias Básicas, Universidad Católica del Maule, Talca, Chile

³ Laboratorio de Comunicación Animal, Departamento de Biología y Química, Facultad de Ciencias Básicas, Universidad Católica del Maule, Talca, Chile

can promote a stable dynamical pattern in the consumer-resource interaction depending on both the magnitude of the energy allocation change and the time lag between environmental sensibility instants and when the expression of the plastic trait occurs.

Keywords Energy allocation · Population dynamics · Phenotypic plasticity and Consumer-resource model

Mathematics Subject Classification 92B05 · 34A37

1 Introduction

The habitats of numerous species have undergone profound transformations due to a series of environmental changes, affecting considerably both intraspecific and interspecific relationships (Bellard et al. 2012). A potential outcome is a decoupling between the organisms' adaptations and their environment (Peñuelas et al. 2013). In response to environmental changes, organisms are expected to disperse, searching for more proper environments. When dispersion is not possible, populations may adapt to novel environments through genetic changes (Fox et al. 2019). Nevertheless, if the rate of environmental change cannot be followed by adaptive change, the occurrence of phenotypic plasticity may be the only way to overcome the risks of extinction (Wong and Candolin 2014; Chevin et al. 2010; Hoffmann and Sgrò 2011).

Phenotypic plasticity is defined as the ability of an organism (or genotype) to change in characteristics such as behavior, morphology, or physiology in response to different environmental conditions (Pigliucci 2005; West-Eberhard 2008). Adaptive phenotypic plasticity provides organisms a greater probability of surviving in the novel, changing, and increasingly adverse environments, a term denominated plastic rescue (Chevin and Hoffmann 2017; Fox et al. 2019). The success of phenotypic plasticity resulting from an adaptive response is strongly dependent on reliable cues, *i.e.*, environmental information, that promotes the expression of a phenotype which leads to increased fitness. Nevertheless, it should also consider the existence of costs associated with the capability of plastic responses (Bonamour et al. 2019; DeWitt et al. 1998; Auld et al. 2010; Murren et al. 2015; Van Kleunen and Fischer 2005).

Understanding the role of phenotypic plasticity in consumer-resource interactions (such as predator-prey, plant-herbivore, and host-parasite relationships) has been of great interest to evolutionary ecologists and theoretical mathematical modelers (Getz 2011, 2012). According to Agrawal (2001), the intersection between these two approaches has allowed a deeper insight into the mechanisms underlying the maintenance of these interspecific interactions. Following a theoretical approach and subsequent empirical validation, DeLong et al. (2014) incorporated the body size in a predator-prey relationship as a plastic trait that change across generations. In addition, the optimal values resulted from matching the expected environmental supply of resources (defined from per capita consumption) and the predator resource demand (corresponding to the maximum ingestion rate). Body size is a relevant measure in organisms' life history due to its high correlation with several life-history parameters (Blueweiss et al. 1978). Furthermore, previous researches studying adaptive plasticity

in different contexts show that environmental changes produce changes through the ontogeny stabilizing role on the consumer-resource dynamics (Takimoto 2003) and also may have effects on the population fitness in plant-herbivore interactions (Thiel et al. 2021).

The life history is the general pattern of growth, reproduction, and survival of organisms, and results from the allocation strategies of limited energetic resources towards different vital functions (Alonzo and Kindsvater 2008). Thus, the life-history strategy of organisms is governed by cost/benefit rules and is expected to evolve to maximize the organism's fitness, which is commonly measured by the growth reproductive rate r or by the net reproduction \mathcal{R}_0 (de Roos et al. 2008; Heino and Kaitala 1999). The definition of the life history of organisms from the bioenergetic of view has allowed investigating the optimal investment patterns on dynamic behaviors of consumers and resources as foraging/reproduction (Akhmetzhanov et al. 2011) or foraging/diapause associations (Staňková et al. 2012, 2013; Stankova et al. 2013). In addition, this approach has also allowed the understanding of how the energy obtained from consumed resources is allocated to growth, reproduction, maintenance, or storage depending on particular traits (e.g., the body size of organisms) (Kozłowski and Wiegert 1986; Ziółko and Kozłowski 1983; Engen and Saether 1994), environmental conditions (e.g., constant, deterministic or stochastic environments) (Perrin and Sibly 1993; Fischer et al. 2009, 2010) and evaluate its effect on interspecific relationships (e.g., consumer-resource dynamics) (Gutiérrez et al. 2020).

Phenotypic expression of the plasticity is dependent strongly on the degree of environmental heterogeneity (Fischer et al. 2009, 2010). In the literature, there are three life-history strategies concerning energy allocation, which are obtained both from empirical and theoretical approaches. Firstly, Ellers and van Alphen (1997) using an experimental approach in the parasitoid *Asobara tabida*, tested the hypothesis that fat reserves are invested for both survival and reproduction. These authors showed that the resources allocated to reproduction decrease in the presence of low food abundance. Secondly, the results of Stelzer (2001) show that common planktonic rotifer *Synchaeta pectinata* increases the energy allocated to reproduction as food becomes more limited. This life-history strategy emerges from the low probability that an individual survives until the next egg deposition as available food reduces. Thirdly, from a theoretical approach, Fischer et al. (2009) reconciles these two opposite predictions. In a stochastic environment, where the availability of individual resources is a random variable that is assumed as an environmental variable, the reproductive investment is promoted at the extreme ends of the environmental gradient, namely when available resources increase or decrease.

The relationship between phenotypic plasticity and population growth has been studied in various investigations which consider a wide variety of environments (e.g., stochastic and deterministic) to evaluate the premise of the plastic rescue with a focus on the persistence and stability of populations both isolated and interacting with others (Chevin et al. 2010; Chevin and Lande 2010; Reed et al. 2010; Ashander et al. 2016; Kovach-Orr and Fussmann 2012). Here, we formulate a basic consumer-resource model in which the energy allocation toward reproduction vs. maintenance as a plastic trait is incorporated. Our purpose is to analyze whether the allocation strategies defined by both positive and negative feedback between the availability of

resources and energy investment in reproduction promote the stable behavior of the consumer-resource dynamics. This dynamical pattern corresponds to trajectories stable converging to a long-term equilibrium value. The energy investing in reproductive tasks is a fraction of the consumer's internal energy, which is modeled through the energetic trade-off between individual consumption of resources and maintenance costs. Incorporating the consumer's internal energy in consumer-resource interaction is commonly a simple way and effective to modify the phenomenological modeling approach of the consumer-resource models and thus transform it into a mechanistic modeling approach, which now incorporates the individual level (Kooijman 2000).

It is widely documented that the plastic responses of the organisms are usually induced, both directly and indirectly, by multiple environmental variables (usually correlated) that provide reliable information about the selective environment in which the determined phenotypic trait will be expressed (Schlaepfer et al. 2002; Miner et al. 2005), existing a time lag between phenotypic determination and trait expression (Bonamour et al. 2019; Chevin and Lande 2015). Thus, in Sect. 2 we will introduce our mathematical model for consumer-resource interaction based on impulsive differential equations, (Lakshmikantham et al. 1989; Samoilenko and Perestyuk 1995), which has also been denominated semi-discrete models (Mailleret and Lemesle 2009), and characterized by combining continuous and discrete time-scale processes under at same dynamics. In this approach, the modeling of continuous processes carries out through ordinary differential equations whose dynamic is abruptly modified at specific times employing jump or impulse conditions according to a discrete evolution rule. Indeed, we introduced two moments of impulsive effects associated with instants at which consumer individuals obtain environmental information and when energy allocation strategy change occurs. Between these instants, at a continued time-scale, the consumption process occurs through which both the decrease in resource density and the increase of the consumer biomass (Ramos-Jiliberto 2005). In the Sect. 3 we will present our results through a comparative analysis between plastic and non-plastic temporal dynamics, obtained from an analytical and numerical investigation with an emphasis on the magnitude of energy allocation change, the time lag between environmental sensibility instants and when expression of phenotypic plasticity occurs, and the phenotypic plasticity costs in relation to the promotion of the stable pattern. Finally, our findings are discussed in Sect. 4 joint to possibilities for future work. Technical details are described in the appendix.

2 Consumer-resource model with plastic energy allocation

Our model considers a consumer-resource interaction where the resource is an energy source for the consumer individuals. The energy is allocated in both reproduction and maintenance as a function of the variation of resource availability. As a first approximation for mathematical modeling, we assumed that variation of the available resource provides reliable information about future selection on the strategy of energy allocation at the instants $s_n = n\tau$ and which expressed at the instants $\tau_n = s_n + l\tau$ with $n = 0, 1, 2, \dots$, $0 < l < 1$ and $\tau > 0$, for either favor reproduction or maintenance.

Individuals have a piecewise constant energy allocation strategy over time. The ability to be plastic involves the emergence of various types of costs. In particular, we consider phenotypic plasticity costs of maintenance (Bonamour et al. 2019; DeWitt et al. 1998; Auld et al. 2010; Murren et al. 2015; Van Kleunen and Fischer 2005).

2.1 Consumer-resource model

From the classical mathematical formulation based on ordinary differential equations (also valid for difference equations), the consumer-resource interaction is usually modeled either by the Individual Survival or Biomass Conversion (BC) principles. These approaches are differentiated mainly in the mathematical expression used to represent the per capita growth rate of consumers (Ramos-Jiliberto 2005), formulating a wide assortment of mathematical models that have been the subject of extensive studies in theoretical population ecology (Arditi and Ginzburg 1989; Arditi and Berryman 1991; Berryman 1992; Rosenzweig 1971; Getz 1984, 2009) and the mathematical theory of dynamic systems (González-Olivares et al. 2011a, b; González-Olivares and Rojas-Palma 2013).

Particularly, for the consumer-resource models based on the BC principle, the reproduction of consumers is resource consumption dependent. The resource extraction process involves decreased resource density and consumer biomass increase, mathematically represented respectively by the functional and numeric responses (see Fig. 1(a)). However, in the cycle-life of organisms, the consumed resource is an energy source that should not only be invested in reproduction but also in foraging, maintenance, or storage (Fischer et al. 2009, 2010; Boggs 1992).

Including the life history of organisms in a modeling framework implies focusing on processes at the individual level (Kooijman 2000). A simple way to incorporate the individual level into the consumer-resource interaction has been to include an intermediate state representing the organism's internal energy $e = e(t)$; in our case, this energy is associated with consumer organisms (Akhmetzhanov et al. 2011; Staňková et al. 2012, 2013; Stankova et al. 2013; Gutiérrez et al. 2020; Sun and de Roos 2015, 2017; Sun et al. 2020; Soudijn and de Roos 2016).

Let be $x(t)$ and $y(t)$ two measures of abundance for the resource and consumer populations at time $t \geq 0$, respectively. Consumer individuals allocate their internal energy toward reproduction in the fraction $\alpha = \alpha(t)$ ($0 \leq \alpha \leq 1$) and the remaining part, $1 - \alpha$, is destined for maintenance such that

$$e := e_r + e_m = \alpha e + (1 - \alpha)e.$$

Therefore, we propose the following consumer-resource model based on the BC principle (see Fig. 1(b))

$$\begin{cases} x' = g(x, y)x - \phi(e_m)h(x, y)y, \\ e' = -\varphi(\alpha)e + b\phi(e_m)h(x, y), \\ y' = f(e_r)y, \end{cases} \quad (1)$$

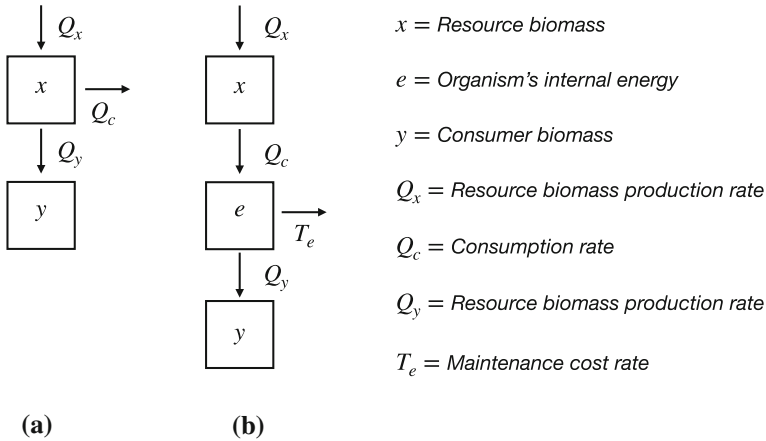


Fig. 1 Schematic of consumer-resource model flows **(a)** traditional ($x \rightarrow y$) and **(b)** modified ($x \rightarrow e \rightarrow y$). On the one hand, from traditional schema $x' = Q_x - Q_c = g(x, y)x - \phi h(x, y)y$ and $y' = Q_y = f(Q_c)y$ are obtained. On the other hand, from modified schema $x' = Q_x - Q_c$, $e' = Q_c - T_e$ and $y' = Q_y = f(e)y$. Here, $g(\cdot)$ is the per capita growth function of the resources, $h(\cdot)$ is the per-consumer extraction rate of resources, and $f(\cdot)$ is the conversion function from the consumption resource/organism's internal energy to the per capita consumer population growth

where $g(x, y)$ is the per capita growth function of the resources, $h(x, y)$ is the per-consumer extraction rate of resources, namely the functional response, and $f(e_r)$ is the conversion function from the reproduction energy to the per capita consumer population growth. For more details, consult Ramos-Jiliberto (2005). Furthermore, $\varphi(\alpha)$ is the maintenance cost of consumer per unit individual energy, and $\phi(e_m)$ is the efficiency of predation of the consumers with the basic properties:

$$\phi(0) = 0, \quad \phi(+\infty) = \phi_0 > 0, \quad \text{and} \quad \frac{d\phi}{de_m}(e_m) > 0.$$

Finally, $b > 0$ is the efficiency of conversion of the resource to consumers' internal energy.

First, we assumed that the per capita growth rate of resources is density-independent and described by $g(x, y) = r$, where $r > 0$ is the intrinsic resource growth rate. This principle is adopted from Takimoto (2003), due to assuming growth of resources is logistic type, inherently entails a stabilizing effect on the consumer-resource dynamic. Second, an adequate function for representing the per capita growth of the consumer population, linear with respect to the reproduction energy, is given by

$$f(e_r) = \rho\{e_r - \delta\} = \rho\{\alpha e - \delta\} = f(e, \alpha), \tag{2}$$

where $\rho > 0$ is the maximum per capita growth rate of the consumer population and $\delta > 0$ is the reproduction energy level needed to maintain a zero growth rate. Note

that in the absence of energy destined for reproductive functions, an abrupt decline in the consumer population is obtained. Third, the efficiency of predation is given by

$$\phi(e_m) = \frac{\phi_0 e_m}{e_0 + e_m} = \frac{\phi_0(1 - \alpha)e}{e_0 + (1 - \alpha)e} = \phi(e, \alpha),$$

where e_0 is the maintenance energy at which the predator efficiency reaches one-half ϕ_0 . Fourth, the maintenance cost of consumer per unit individual energy is the linear type and described by $\varphi(\alpha) = \varphi_r \alpha + \varphi_m(1 - \alpha)$ where $\varphi_i > 0$ are denominated weights for $i \in \{r, m\}$. Note that $\varphi(\alpha)$ increases as energy allocation favors reproduction (as $\alpha \rightarrow 1$) with φ_r as the maximum value. Finally, the per-consumer extraction rate of resources is assumed proportional to the abundance of resources, $h(x, y) = ax$ with $a > 0$ which is a measure of the resource quality. Therefore, the following particular model is obtained

$$X_\eta : \begin{cases} x' = rx - \frac{\phi_0(1 - \alpha)e}{e_0 + (1 - \alpha)e}axy, \\ e' = -\varphi(\alpha)e + b \frac{\phi_0(1 - \alpha)e}{e_0 + (1 - \alpha)e}ax, \\ y' = \rho\{\alpha e - \delta\}y, \end{cases} \tag{3}$$

where $\eta = (r, a, \phi_0, e_0, \varphi_r, \varphi_m, b, \rho, \delta) \in \mathbb{R}_+^9$ with $\varphi_m < \varphi_r$.

The parameters of the model (3) have ecological meanings that as a summary are described in Table 1 along with other parameters associated with plastic energy allocation to come soon.

As is traditional to simplify the calculations, we also carry out a change of variables and a time re-scaling which is given by the function

$$p(u, v, w, s) = \left(u, e_0v, \frac{rw}{a\phi_0}, \frac{s}{r}\right) = (x, e, y, t),$$

and conveniently transforming the parameters:

$$\varphi_m = r\tilde{\varphi}_m, \varphi_r = r\tilde{\varphi}_r, ab\phi_0 = re_0\tilde{b}, \rho e_0 = r\tilde{\rho}, \text{ and } \delta = e_0\tilde{\delta},$$

we obtained an equivalent system to (3) and given by $\tilde{X}_\psi = p \circ X_\eta$, or equivalently

$$\tilde{X}_\psi : \begin{cases} u' = u - \frac{(1 - \alpha)v}{1 + (1 - \alpha)v}uw, \\ v' = -\tilde{\varphi}(\alpha)v + \tilde{b} \frac{(1 - \alpha)v}{1 + (1 - \alpha)v}u, \\ w' = \tilde{\rho}\{\alpha v - \tilde{\delta}\}w, \end{cases} \tag{4}$$

where $\psi = (\tilde{\varphi}_r, \tilde{\varphi}_m, \tilde{b}, \tilde{\rho}, \tilde{\delta}) \in \mathbb{R}_+^5$ and $\tilde{\varphi}(\alpha) = \tilde{\varphi}_r \alpha + \tilde{\varphi}_m(1 - \alpha)$ with $\tilde{\varphi}_m < \tilde{\varphi}_r$.

Table 1 Parameters meanings of models (3), (4), and (7). The first block shows the parameters of models (3) and (4), and the second block has which are additionally used in the model (7)

Parameter	Ecological meaning	Brief name for figures
r	Intrinsic resource growth rate.	
ϕ_0	Maximum predator efficiency.	
e_0	Maintenance energy at which predator efficiency reaches one-half ϕ_0 .	
a	Measure of the resource quality.	
$\varphi_r, \varphi_m, \tilde{\varphi}_r, \tilde{\varphi}_m$	Weights of maintenance cost of consumer per unit individual energy associated with reproduction and survival life-history functions.	Reproduction and survival weights.
b, \tilde{b}	Efficiency of conversion of the resource to consumers internal energy.	
$\rho, \tilde{\rho}$	Maximum per capita growth rate of consumer population.	Consumer intrinsic growth.
$\delta, \tilde{\delta}$	Reproduction energy level needed to maintain a zero growth rate.	Reproductive energy for steady-state.
τ^{-1}	Environmental sensibility frequency.	τ : Inter-period of environmental sampling.
l	Fraction of inter-period of environmental sampling that defines the time lag between the inducing environment and the selective environment, $l\tau$.	Lag fraction.
σ_0	Maximum magnitude of the energy allocation change when the anticipatory information is absent.	Response of anticipation to null information.
θ	Sensibility to the anticipatory information.	
U_0^{-1}	Energy allocation sensibility to the variation net of the available resource.	U_0 : Reciprocal of energy allocation sensibility.
c	Plasticity maintenance cost rate.	Plasticity cost.

2.2 Plastic energy allocation

Let be $s_n = n\tau$ a sequence of instants at which the organisms obtain environmental information, where $n = 0, 1, 2, \dots$ and $\tau > 0$. Thus, energy allocation change occurs $l\tau$ units time after environmental sensibility occurred which results in a new phenotypic value of energy allocation at instants $\tau_n = s_n + l\tau$ where $l \in (0, 1)$. Let be $\alpha(s) = \alpha(s, u(s)) \in [0, 1]$ the energy allocation toward reproduction, a function that quantifies the phenotypic expression of plasticity according to the available resource. We proposed that $\alpha(s)$ is a piecewise constant function (does not affect to get (4) from (3)) and solution of impulsive differential equation:

$$\begin{cases} \alpha'(s) = 0 & , \text{ if } s \neq \tau_n, \\ \alpha(s^+) = \alpha(s) + G(z(s)) & , \text{ if } s = \tau_n. \end{cases} \tag{5}$$

where $\alpha(s^+) = \lim_{q \rightarrow s^+} \alpha(q)$ and $G(\cdot)$ is the magnitude of energy allocation change and $z(s) = (u(s), u(s - l\tau), u'(s), \alpha(s))$.

The impulsive component of equation (5) is mainly formulated in function to $\Delta u(s) := u(s) - u(s - l\tau)$ at $s = \tau_n$. Considering that the phenotypic plasticity expression is usually represented by a linear type function and measured by its slope (Chevin and Lande 2010), we assumed $\alpha(s) = \beta \cdot u(s) + \gamma$. On the one hand, the solution of equation (5) is $\alpha(s) = \alpha(\tau_n^+)$ for any $s \in (\tau_n, \tau_{n+1}]$. In particular, $\alpha(s_n) = \alpha(\tau_n)$ is obtained for each $n \geq 0$. On the other hand, $\alpha(\tau_n^+) = \beta \cdot u(\tau_n^+) + \gamma = \beta \cdot u(\tau_n) + \gamma$, and $\alpha(\tau_n) = \alpha(s_n) = \beta \cdot u(s_n) + \gamma$. Therefore, $\alpha(\tau_n^+) - \alpha(\tau_n) = \beta \cdot \{u(\tau_n) - u(s_n)\}$, or equivalent, $G(z(\tau_n)) = \beta \cdot \Delta u(\tau_n)$. According to positive feedback, $\beta > 0$ (and the otherwise, negative feedback, $\beta < 0$), at $s = \tau_n$ we have:

i) If $\Delta u(\tau_n) \geq 0$ then $\alpha(\tau_n) \leq \alpha(\tau_n^+) < 1$. Therefore,

$$G(z(\tau_n)) = \beta \Delta u(\tau_n) < 1 - \alpha(\tau_n).$$

Thus, there exist $0 < \epsilon_1 < 1$ such that $G(z(\tau_n)) = \epsilon_1(1 - \alpha(\tau_n))$, and

ii) If $\Delta u(\tau_n) \leq 0$ then $0 < \alpha(\tau_n^+) \leq \alpha(\tau_n)$. Therefore,

$$G(z(\tau_n)) = \beta \Delta u(\tau_n) > -\alpha(\tau_n).$$

Thus, there exist $0 < \epsilon_2 < 1$ such that $G(z(\tau_n)) = -\epsilon_2\alpha(\tau_n)$.

For simplicity, we assume that $\epsilon_1 = \epsilon_2 = \epsilon$. With the aim of incorporating both retrospective and anticipating information, ϵ is a function dependent $\Delta u(\tau_n)$ and $u'(\tau_n)$ based on a multiplicative form. Note that $\Delta u(\tau_n)$ is the net variation of available resource in the temporal range $[s_n, \tau_n]$, and $u'(\tau_n)$ is the instantaneous variation of available resource which indicates qualitatively the future availability of food. Thus, we propose $\epsilon = \sigma(u'(\tau_n)) \cdot \mu(|\Delta u(\tau_n)|)$, where

$$\sigma(u'(\tau_n)) = \frac{\sigma_0}{\sigma_0 + (1 - \sigma_0)e^{-\theta u'(\tau_n)}}, \quad \text{and} \quad \mu(|\Delta u(\tau_n)|) = \frac{U_0^{-1}|\Delta u(\tau_n)|}{1 + U_0^{-1}|\Delta u(\tau_n)|},$$

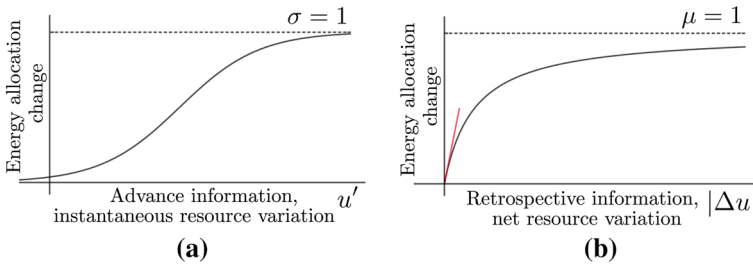


Fig. 2 Component functions of magnitude of the energy allocation change, **(a)** $\sigma = \sigma(u'(\tau_n))$ described by a logistic curve and **(b)** $\mu(|\Delta u(\tau_n)|)$ described by a hyperbolic curve. Here, the red line is $y = U_0^{-1}|\Delta u(\tau_n)|$ (color figure online)

with $\theta \geq 0, 0 < \sigma_0 < 1$, and $U_0 > 0$ (see Fig. 2). Here, σ_0 is the maximum magnitude of the energy allocation change when the anticipatory information is absent (*i.e.*, $\theta = 0$), and U_0^{-1} is the energy allocation sensibility to the variation net of the available resource (*i.e.*, $\mu'(|\Delta u(\tau_n)|)$ at $|\Delta u(\tau_n)| = 0$). Consequently, as U_0^{-1} increases, the influence of $|\Delta u(\tau_n)|$ on the energy allocation change $G(z(\tau_n))$ increases too.

Therefore, the mathematical expression proposed for modeling the energy allocation change is given by

$$G(z(\tau_n)) = \frac{\sigma_0}{\sigma_0 + (1 - \sigma_0)e^{-\theta u'(\tau_n)}} \cdot \frac{U_0^{-1}|\Delta u(\tau_n)|}{1 + U_0^{-1}|\Delta u(\tau_n)|} \cdot \left(\frac{1 + (-1)^{\mathcal{H}(\tau_n)}}{2} - \alpha(\tau_n) \right), \tag{6}$$

where

$$\mathcal{H}(\tau_n) = \begin{cases} 1 - H(\Delta u(\tau_n)) & , \text{ for positive feedback.} \\ H(\Delta u(\tau_n)) & , \text{ for negative feedback.} \end{cases}$$

and H is the Heaviside step function.

Fig 3, illustrates the recursive dependence of $\alpha(\tau_n)$ on $\alpha(\tau_n^+)$ according to sign of $\Delta u(\tau_n)$. The energy allocation strategy value changes as much as it “jumps” between the values $\alpha(\tau_n^+) = (1 - \epsilon)\alpha(\tau_n) + \epsilon$ and $\alpha(\tau_n^+) = (1 - \epsilon)\alpha(\tau_n)$, reaching an equilibrium value when it satisfies the relation $\alpha(\tau_n^+) = \alpha(\tau_n)$, *i.e.*, $G(z(\tau_n)) \equiv 0$ for any $n \geq N$ and some $N > 0$. Therefore, the stabilization of the plastic phenotype is a consequence of the dynamics underlying the consumer-resource interaction, whose dynamic pattern is dampened by the variation in available resources. In the long term, the phenotypic expression of plasticity is absent.

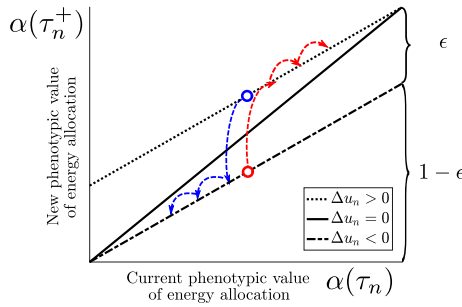


Fig. 3 Recursive relation between the new and current phenotypic value of energy allocation, given by $\alpha(\tau_n^+)$ and $\alpha(\tau_n)$ respectively, for $n = 0, 1, 2, \dots$ according to net variation of available resource $\Delta u_n = u(\tau_n) - u(s_n)$ in the positive feedback, where $s_n = n\tau$ and $\tau_n = s_n + l\tau$. Here, the dot line is $\alpha(\tau_n^+) = (1 - \epsilon)\alpha(\tau_n) + \epsilon$, the continuous line is $\alpha(\tau_n^+) = \alpha(\tau_n)$, and the dashed line is $\alpha(\tau_n^+) = (1 - \epsilon)\alpha(\tau_n)$ where $\epsilon = \epsilon(u'(\tau_n), \Delta u_n) \in (0, 1)$. The blue arrow (the contrary, red arrow) represents the energy allocation change from $\Delta u_n > 0$ to $\Delta u_n < 0$ according to positive feedback (color figure online)

2.3 The model

In the consumer-resource dynamic given by model (4), the resource level $u(s_n)$ induces the development of energy allocation strategy $\alpha \in [0, 1]$ expressed $l\tau$ time-unit later at the resource level $u(s_n + l\tau) = u(\tau_n)$. The time lag between the inducing environment and the selective environment is $l\tau := \tau_n - s_n$. The plasticity phenotypic expression depends on the variation of resource, both net and instantaneous, according to a linear norm reaction (Chevin and Lande 2010; Nijhout 2003; Giuseppe and Minelli 2010). Based on the mathematical modeling performed in the previous subsections, the following impulsive mathematical model is proposed

$$\begin{cases} \alpha'(s) = 0 \\ \left. \begin{aligned} u'(s) &= u(s) - \frac{[1 - \alpha(s)]v(s)}{1 + [1 - \alpha(s)]v(s)} u(s)w(s) \\ v'(s) &= -\tilde{\varphi}(\alpha(s))v(s) + \tilde{b} \frac{[1 - \alpha(s)]v(s)}{1 + [1 - \alpha(s)]v(s)} u(s) \\ w'(s) &= \tilde{\rho}\{\alpha(s)v(s) - \tilde{\delta}\}w(s) \end{aligned} \right\} \text{if } s \notin \{s_n, \tau_n\}, \\ Y_\xi : \left. \begin{aligned} \alpha(s^+) &= \alpha(s) \\ u(s^+) &= u(s) \\ v(s^+) &= (1 - c)v(s) \\ w(s^+) &= w(s) \end{aligned} \right\} \text{if } s = s_n, \\ \left. \begin{aligned} \alpha(s^+) &= \alpha(s) + G(u(s), u(s - l\tau), u'(s), \alpha(s)) \\ u(s^+) &= u(s) \\ v(s^+) &= v(s) \\ w(s^+) &= w(s) \end{aligned} \right\} \text{if } s = \tau_n, \end{cases} \tag{7}$$

where $\xi = (\tau, \tilde{\varphi}_r, \tilde{\varphi}_m, \tilde{b}, \tilde{\rho}, \tilde{\delta}, U_0, \theta, \sigma_0, l, c) \in \mathbb{R}_+^8 \times (0, 1)^2 \times [0, 1]$ with $\tilde{\varphi}_m < \tilde{\varphi}_r$. Here, $\alpha(s^+)$, $u(s^+)$, $v(s^+)$, and $w(s^+)$ represent the energy allocation strategy, resource biomass, consumers energy, and consumers biomass immediately after the environmental sensibility or energy allocation change occurred. According to Van Kle-

unen and Fischer (2005), a cost of plasticity is the reduction in fitness of a genotype as a consequence of expressing a certain phenotype through plastic rather than fixed development (Van Kleunen and Fischer 2005). Both reproduction and survival depend on the organism's internal energy, functions that define its fitness. Thus, we assumed that phenotypic plasticity demands maintenance costs due to the use of sensory or regulatory systems necessary to acquiring information about the environment and respond to environmental conditions (Bonamour et al. 2019; DeWitt et al. 1998; Auld et al. 2010; Murren et al. 2015; Van Kleunen and Fischer 2005). This cost is a fraction $0 \leq c < 1$ of the organism's internal energy which is paid at instants $s = s_n$.

3 Results

We performed a preliminary analysis of the non-plastic case, *i.e.* when the energy allocation is a constant value over time and without changes in resource availability. Parametric conditions that guarantee stable and unstable temporal dynamics in the long term are found. The stable pattern is intrinsically related to a set of energy allocation values, which we termed the stability range. Because of phenotypic plasticity, stable and unstable patterns emerge depending on the energy allocation strategy adopted (*i.e.*, positive or negative feedback). Considering the number of parameters involved in the impulsive mathematical model (7), given by the set ξ , numerical and descriptive analyses of temporal dynamics were carried out to assess: the magnitude of the energy allocation change, time lag between environmental sensibility and phenotypic expression, and maintenance plasticity phenotypic costs.

3.1 Non-plastic case

In this case, the consumer-resource dynamics is given by system (4). Thus, in order to transform the rational system (4) in a polynomial system, we consider the following time re-scaling

$$\bar{\tau} = \int_0^s [1 + (1 - \alpha)v(k)]^{-1} dk.$$

Therefore, the following polynomial system of degree three is obtained

$$Z_\psi : \begin{cases} \dot{u} = \{1 + (1 - \alpha)v - (1 - \alpha)vw\}u, \\ \dot{v} = \{-\tilde{\varphi}(\alpha)[1 + (1 - \alpha)v] + \tilde{b}(1 - \alpha)u\}v, \\ \dot{w} = \tilde{\rho}[1 + (1 - \alpha)v]\{\alpha v - \tilde{\delta}\}w, \end{cases} \quad (8)$$

where \dot{u} , \dot{v} and \dot{w} are derivatives with respect to $\bar{\tau}$.

3.1.1 Equilibrium points and local behavior

The equilibrium solutions of the system (8) must satisfy the algebraic equations $\dot{u} = 0$, $\dot{v} = 0$, and $\dot{w} = 0$. Depending on $\alpha \in [0, 1]$ the following equilibrium solutions are obtained.

- (a) If $\alpha \in \{0, 1\}$ then $P_0 = (0, 0, 0)$, and
- (b) If $\alpha \in (0, 1)$ then $P_0 = (0, 0, 0)$ and $P_1 = (u^*, v^*, w^*)$ where

$$u^* = \frac{[\alpha + (1 - \alpha)\tilde{\delta}]\tilde{\varphi}(\alpha)}{\alpha(1 - \alpha)\tilde{b}}, \quad v^* = \frac{\tilde{\delta}}{\alpha}, \quad \text{and} \quad w^* = \frac{\alpha + (1 - \alpha)\tilde{\delta}}{(1 - \alpha)\tilde{\delta}}.$$

Then, we can derive the following conclusion.

Proposition 1 *In the system (8),*

- (a) P_0 is a unstable point, and
- (b) If $0 < \tilde{\rho} < \tilde{\rho}_0$, where

$$\tilde{\rho}_0 = \frac{\alpha(1 - \alpha)\tilde{\varphi}(\alpha)}{[\alpha + (1 - \alpha)\tilde{\delta}]^2},$$

then P_1 is a locally asymptotically stable point.

Proof In the first case, the eigenvalues of the linearization matrix around equilibrium point P_0 are $\{1, -\tilde{\varphi}(\alpha), -\tilde{\rho}\tilde{\delta}\}$. In the second case, we checked the conditions of the Routh-Hurwitz criterion on the characteristic equation

$$\lambda^3 + p_2\lambda^2 + p_1\lambda + p_0 = 0, \tag{9}$$

where $p_2 = (1 - \alpha)\alpha^{-1}\tilde{\delta}\tilde{\varphi}(\alpha)$, $p_1 = [1 + (1 - \alpha)\alpha^{-1}\tilde{\delta}]\tilde{\varphi}(\alpha)$, and $p_0 = \tilde{\rho}[1 + (1 - \alpha)\alpha^{-1}\tilde{\delta}]^3\tilde{\delta}\tilde{\varphi}(\alpha)$. Then, $\Delta_1 = p_2 > 0$ and $\Delta_2 = p_2p_1 - p_0 > 0$ if, and only if, $0 < \tilde{\rho} < \tilde{\rho}_0$. □

An important consequence of the Routh-Hurwitz criterion is that its use lets find the parametric conditions for the existence of purely imaginary roots of the characteristic polynomial. Thus, when $\tilde{\rho} = \tilde{\rho}_0$ the roots of characteristic polynomial associated with Jacobian matrix around the equilibrium point P_1 , given by (9) are $\lambda_1 = -p_2$ and $\lambda_{2,3} = \pm\sqrt{p_1}i$.

Proposition 2 *The model (8) has a Hopf bifurcation around the equilibrium point P_1 with bifurcation value is $\tilde{\mu} := \tilde{\rho} - \tilde{\rho}_0 = 0$. Therefore, there exists a family of periodic solutions with a period close to $2\pi/\sqrt{p_1}$ which can be stable or unstable.*

Proof Let be $\lambda = a(\tilde{\rho}) \pm \omega(\tilde{\rho})i$ the complex roots of the polynomial (9) depending on the bifurcation parameter $\tilde{\rho}$. If $\tilde{\rho} = \tilde{\rho}_0$, from Routh-Hurwitz criterion, $a(\tilde{\rho}_0) = 0$

and $\omega(\tilde{\rho}_0) = \sqrt{p_1}$ are obtained. Besides, from the polynomial (9), we have

$$\frac{d\lambda(\tilde{\rho})}{d\tilde{\rho}} = -\frac{p_0}{\tilde{\rho}(3\lambda^2 + 2p_2\lambda + p_1)},$$

it follows that the transversality condition

$$\operatorname{Re} \left(\left. \frac{d\lambda(\tilde{\rho})}{d\tilde{\rho}} \right|_{\tilde{\rho}=\tilde{\rho}_0, \lambda=\sqrt{p_1}i} \right) = \operatorname{Re} \left(\frac{p_0}{2(p_1 - i\sqrt{p_1}p_2)} \right) = \frac{p_0}{2(p_1 + p_2^2)} > 0.$$

Thus, it appears that a Hopf bifurcation occurs at $\tilde{\rho} = \tilde{\rho}_0$. To check the stability of the bifurcating periodic orbits we calculated the first Lyapunov number. Firstly, we translate the equilibrium point $P_1 = (u^*, v^*, w^*)$ to the origin $(0, 0, 0)$ using the transformation $(u, v, w) \rightarrow (U + u^*, V + v^*, W + w^*)$. Then, the system (8) leads to

$$\begin{pmatrix} U' \\ V' \\ W' \end{pmatrix} = \begin{pmatrix} 0 & -\frac{\tilde{\varphi}(\alpha)[\alpha+(1-\alpha)\tilde{\delta}]}{(1-\alpha)\tilde{\delta}\tilde{b}} & -\frac{\tilde{\varphi}(\alpha)[\alpha+(1-\alpha)\tilde{\delta}]\tilde{\delta}}{\alpha^2\tilde{b}} \\ \frac{(1-\alpha)\tilde{b}\tilde{\delta}}{\alpha} & -\frac{(1-\alpha)\tilde{\varphi}(\alpha)\tilde{\delta}}{\alpha} & 0 \\ 0 & \frac{\alpha\tilde{\varphi}(\alpha)}{\tilde{\delta}} & 0 \end{pmatrix} \cdot \begin{pmatrix} U \\ V \\ W \end{pmatrix} + \begin{pmatrix} F \\ G \\ H \end{pmatrix}, \tag{10}$$

where

$$\begin{aligned} F(U, V, W) &= -\frac{\tilde{\delta}}{\alpha}UV \\ &\quad -\frac{(1-\alpha)\tilde{\delta}}{\alpha}UW - \frac{\tilde{\varphi}(\alpha)[\alpha+(1-\alpha)\tilde{\delta}]}{\alpha\tilde{b}}VW - (1-\alpha)UVW, \\ G(U, V, W) &= \tilde{b}(1-\alpha)UV - \tilde{\varphi}(\alpha)(1-\alpha)V^2, \\ H(U, V, W) &= \frac{\alpha(1-\alpha)\tilde{\varphi}(\alpha)}{\alpha+(1-\alpha)\tilde{\delta}} \left\{ \frac{\alpha}{\tilde{\delta}}V^2 + VW + \frac{\alpha(1-\alpha)}{\alpha+(1-\alpha)\tilde{\delta}}V^2W \right\}. \end{aligned}$$

Let be

$$\begin{pmatrix} U \\ V \\ W \end{pmatrix} = \begin{pmatrix} 0 & \alpha+(1-\alpha)\tilde{\delta} & -\tilde{\delta}\tilde{\varphi}(\alpha)\sqrt{\alpha+(1-\alpha)\tilde{\delta}} \\ -(1-\alpha)\tilde{\delta}^2 & 0 & -\tilde{\delta}\tilde{b}\sqrt{\alpha+(1-\alpha)\tilde{\delta}} \\ \alpha^2 & -(1-\alpha)\alpha\tilde{b} & 0 \end{pmatrix} \cdot \begin{pmatrix} X \\ Y \\ Z \end{pmatrix}.$$

Then, system (10) assumes the canonical form

$$\begin{pmatrix} X' \\ Y' \\ Z' \end{pmatrix} = \begin{pmatrix} -p_2 & 0 & 0 \\ 0 & 0 & \sqrt{p_1} \\ 0 & -\sqrt{p_1} & 0 \end{pmatrix} \cdot \begin{pmatrix} X \\ Y \\ Z \end{pmatrix} + \begin{pmatrix} F_1 \\ G_1 \\ H_1 \end{pmatrix}, \tag{11}$$

where $F_1 = F_1(X, Y, Z)$, $G_1 = G_1(X, Y, Z)$ and $H_1 = H_1(X, Y, Z)$ are shown in appendix. There exists a center manifold for the system (11), which can be represented as follows

$$W^c(0) = \{(X, Y, Z) \in \mathbb{R}^3 : X = q(Y, Z), q(0, 0) = 0, Dq(0, 0) = 0\},$$

where the 2-dimensional central manifold at the origin given by

$$q(Y, Z) = q_{20}Y^2 + q_{11}YZ + q_{02}Z^2 + \dots$$

Then, replacing $X = h(Y, Z)$ in the first equation on system (11) we have the following equation

$$(q_{20}Y^2 + q_{11}YZ + q_{02}Z^2 + \dots)' = -p_2(q_{20}Y^2 + q_{11}YZ + q_{02}Z^2 + \dots) + F_1(q_{20}Y^2 + q_{11}YZ + q_{02}Z^2 + \dots, Y, Z).$$

Thus, equalling the coefficients of the terms Y^2 , YZ and Z^2 , it follows that

$$\begin{aligned} q_0 &= \tilde{\varphi}(\alpha)\{4\alpha^5 + 8\alpha^4\alpha_c\tilde{\delta} + \alpha^2\alpha_c^2[(1 + \alpha)^2 + 4\alpha\tilde{\varphi}(\alpha)]\tilde{\delta}^2 + \alpha\alpha_c^3[\alpha_c^2 + 4\alpha\tilde{\varphi}(\alpha)]\tilde{\delta}^3 + \alpha_c^6\tilde{\varphi}(\alpha)\tilde{\delta}^4\}, \\ q_{20}q_0 &= \alpha\alpha_c^2\tilde{b}^2\{3\alpha^4 + \alpha^3\alpha_c[6 + \tilde{\varphi}(\alpha)]\tilde{\delta} + \alpha\alpha_c^2(1 + \alpha + \alpha^2)\tilde{\delta}^2 + \alpha_c^3[(1 - \alpha)^2 - \alpha\tilde{\varphi}(\alpha)]\tilde{\delta}^3\}, \\ q_{11}q_0 &= -\alpha\alpha_c^4\tilde{b}^2\tilde{\delta}\sqrt{\alpha + \alpha_c\tilde{\delta}}\{\alpha^2 + \alpha\alpha_c[1 - \tilde{\varphi}(\alpha)]\tilde{\delta} + \alpha_c^2\tilde{\varphi}(\alpha)\tilde{\delta}^2\}, \\ q_{02}q_0 &= \alpha^2\alpha_c^2\tilde{b}^2\{\alpha^3 + \alpha^2\alpha_c[2 - \tilde{\varphi}(\alpha)]\tilde{\delta} + \alpha\alpha_c^2\tilde{\delta}^2 + \alpha_c^3\tilde{\varphi}(\alpha)\tilde{\delta}^3\}, \end{aligned}$$

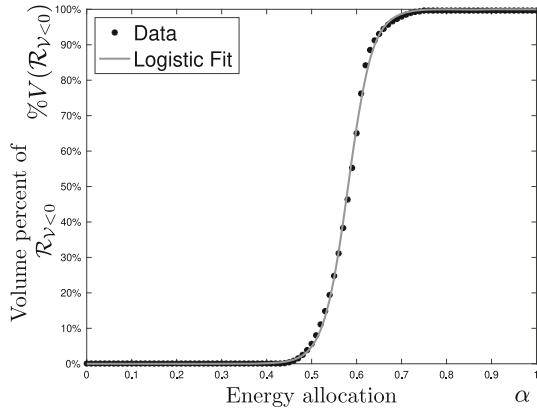
where $\alpha_c = 1 - \alpha$. Therefore, the system (11) restricted to the center manifold is given by

$$\begin{pmatrix} Y' \\ Z' \end{pmatrix} = \begin{pmatrix} 0 & \sqrt{p_1} \\ -\sqrt{p_1} & 0 \end{pmatrix} \cdot \begin{pmatrix} Y \\ Z \end{pmatrix} + \begin{pmatrix} G_2 \\ H_2 \end{pmatrix},$$

where $G_2 = G_1(q(Y, Z), Y, Z)$ and $H_2 = H_1(q(Y, Z), Y, Z)$. Then, the first Lyapunov number is

$$\begin{aligned} \mathcal{V} &= \frac{1}{16} \left(\frac{\partial^3 G_2}{\partial Y^3} + \frac{\partial^3 G_2}{\partial Y \partial Z^2} + \frac{\partial^3 H_2}{\partial Y^2 \partial Z} + \frac{\partial^3 H_2}{\partial Z^3} \right) \\ &+ \frac{1}{16\sqrt{p_1}} \left[\frac{\partial^2 G_2}{\partial Y \partial Z} \left(\frac{\partial^2 G_2}{\partial Y^2} + \frac{\partial^2 G_2}{\partial Z^2} \right) - \frac{\partial^2 H_2}{\partial Y \partial Z} \left(\frac{\partial^2 H_2}{\partial Y^2} + \frac{\partial^2 H_2}{\partial Z^2} \right) - \frac{\partial^2 G_2}{\partial Y^2} \frac{\partial^2 H_2}{\partial Y^2} + \frac{\partial^2 G_2}{\partial Z^2} \frac{\partial^2 H_2}{\partial Z^2} \right], \\ &= \tilde{b}^2 Q(\alpha)/R(\alpha), \end{aligned}$$

Fig. 4 Volume percent of $\mathcal{R}_{\mathcal{V}<0}$, denoted by $\%V(\mathcal{R}_{\mathcal{V}<0})$, according to $\alpha \in (0, 1)$ considering $M = 1$. Note that if $0.76 \lesssim \alpha < 1$ (respectively, $0 < \alpha \lesssim 0.42$) then $\mathcal{V} < 0$ (respectively, $\mathcal{V} > 0$) is obtained for any $(\tilde{\varphi}_r, \tilde{\varphi}_m, \tilde{\delta}) \in (0, 1]^3$ with $\tilde{\varphi}_m < \tilde{\varphi}_r$. In addition, the fit is given by $f(\alpha) = 1/(1 + e^{21.43-36.88\alpha})$



where $Q(\alpha) = a_{16}\alpha^{16} + \dots + a_0$, and $R(\alpha) = b_{12}\alpha^{12} + \dots + b_0$. The coefficients a_j and b_k are in shown in appendix. Note that these coefficients dependent on the parameters $\tilde{\varphi}_r, \tilde{\varphi}_m$ and $\tilde{\delta}$. Consequently, the periodic solution, emanating from equilibrium point P_1 for $\tilde{\rho}$ near $\tilde{\rho}_0$, is stable if $\mathcal{V} < 0$, and is unstable if $\mathcal{V} > 0$. \square

In order to show that both $\mathcal{V} < 0$ and $\mathcal{V} > 0$ are possible, without loss of generality, we can assume $\tilde{b} = 1$ and define for each $\alpha \in (0, 1)$ the following set

$$\mathcal{R}_{\mathcal{V}<0} = \{(\tilde{\varphi}_r, \tilde{\varphi}_m, \tilde{\delta}) \in (0, M]^3 : \mathcal{V} < 0 \text{ with } \tilde{\varphi}_m < \tilde{\varphi}_r\},$$

for some $M > 0$, and the function $\alpha \rightarrow \%V(\mathcal{R}_{\mathcal{V}<0})$ that represents the percentage at which corresponding to the volume of the set $\mathcal{R}_{\mathcal{V}<0}$ with respect to the admissible volume $0.5M^3$ (see Fig. 4).

3.1.2 Stability range

From Proposition 1, stability (at least locally) in the long-term consumer-resource dynamics is guaranteed if the inequality

$$\tilde{\rho} < \tilde{\rho}_0(\alpha) = \frac{\alpha(1 - \alpha)[\tilde{\varphi}_r\alpha + \tilde{\varphi}_m(1 - \alpha)]}{[\alpha + (1 - \alpha)\tilde{\delta}]^2}, \tag{12}$$

is fulfilled. Fixing $(\tilde{\varphi}_r, \tilde{\varphi}_m, \tilde{\delta}, \tilde{\rho}) \in \mathcal{Y} := \{(\tilde{\varphi}_r, \tilde{\varphi}_m, \tilde{\delta}, \tilde{\rho}) \in \mathbb{R}_+^4 : \tilde{\varphi}_m < \tilde{\varphi}_r\}$, the inequality (12) is equivalent to obtain that

$$P(\alpha) = A_3\alpha^3 + A_2\alpha^2 + A_1\alpha + A_0 > 0, \quad \alpha \in (0, 1),$$

where $A_3 = -(\tilde{\varphi}_r - \tilde{\varphi}_m)$, $A_2 = -\tilde{\rho}(1 - \tilde{\delta})^2 - 2\tilde{\varphi}_m + \tilde{\varphi}_r$, $A_1 = -2\tilde{\rho}(1 - \tilde{\delta})\tilde{\delta} + \tilde{\varphi}_m$ and $A_0 = -\tilde{\rho}\tilde{\delta}^2$. By the method of Descartes, it follows that the polynomial P always has a negative root, which allows defining the set

$$\Gamma = \{(\tilde{\varphi}_r, \tilde{\varphi}_m, \tilde{\delta}, \tilde{\rho}) \in \mathcal{Y} : \text{The polynomial } P \text{ has two roots on interval } (0, 1)\},$$

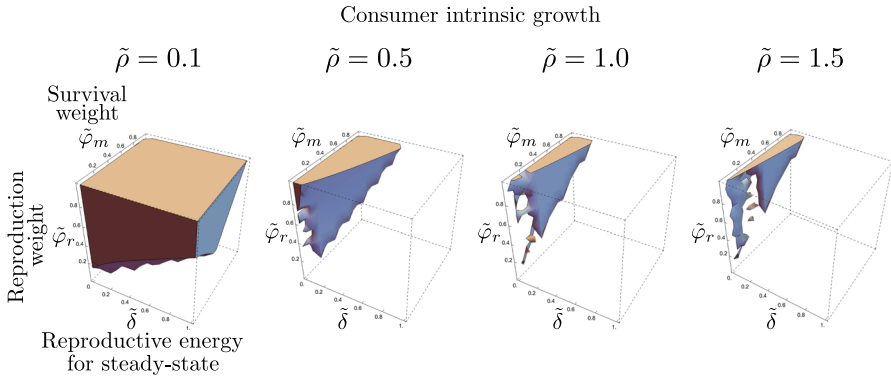


Fig. 5 Parameter combinations of reproductive energy of steady-state $\tilde{\delta}$, reproduction weight $\tilde{\varphi}_r$ and survival weight $\tilde{\varphi}_m$ for different values of the consumer intrinsic growth rate $\tilde{\rho}$. Here, the sets $(0, 1)^3 \times \{\tilde{\rho}\} \cap \Gamma$ with $\tilde{\rho} \in \{0.1, 0.5, 1.0, 1.5\}$. Note that as $\tilde{\rho}$ increases, the volume of these sets decreases

with subsets visible in Fig 5. Therefore, for each $x \in \Gamma$ and initial state $Z_0 = (u_0, v_0, w_0) \in \mathbb{R}_+^3$ of $Z_\psi(t, Z_0)$, the solution of the system (8), there exists an interval

$$l_x := \left\{ \alpha \in (0, 1) : \lim_{t \rightarrow +\infty} Z_\psi(t, Z_0) = P_1(\alpha) \right\}, \tag{13}$$

$$\subseteq L_x := \{ \alpha \in (0, 1) : \tilde{\rho} < \tilde{\rho}_0(\alpha) \},$$

denominated stability range and whose length is denoted by $|l_x|$. Here, L_x corresponds to the maximal stability range. Importantly, the fact that $|l_x|$ depends on Z_0 is because P_1 is a locally asymptotically stable point. It is clear that if Z_0 is taken near to P_1 then the stability range l_x is similar to the maximal stability range L_x (see Fig. 6(a)). The procedure for finding the stability range (13) is summarized in Procedure 1 (see appendix).

Fig 6(b) presents the equivalence between positivity of polynomial P and existence of range L_x , and Figure 6(c) illustrates the graphical relationship of stability condition (12) in the interval $(0, 1)$. From this figure is observed that: First, as $\tilde{\delta}$ increases the plot of $\tilde{\rho}_0$ shrinks due to $\partial \tilde{\rho}_0 / \partial \tilde{\delta} < 0$. Consequently, the horizontal line $y = \tilde{\rho}$ will exceed to $\tilde{\rho}_0$ for any $\alpha \in (0, 1)$ implying that L_x will vanish. Second, as $\tilde{\varphi}_r$ increases is promote the inequality (12) due to distance between $y = \tilde{\rho}$ and $\tilde{\rho}_0$ increases, here $\partial \tilde{\rho}_0 / \partial \tilde{\varphi}_r > 0$. Therefore, this implies that L_x is expanding and $|L_x|$ increasing. The same result is obtained whether as $\tilde{\varphi}_m$ increases, which follows of using the transformation of allocation reverse $\beta \rightarrow 1 - \alpha$ and the symmetry between $\tilde{\rho}_0(\alpha)$ and $\tilde{\rho}_0(1 - \alpha)$ for any $\alpha \in (0, 1)$ with respect to the axis $\alpha = 1/2$. Finally, as $\tilde{\rho}$ increases the horizontal line $y = \tilde{\rho}$ moves vertically, exceeding the function $\tilde{\rho}_0$, which implies $|L_x|$ tends to zero. Additionally, taking $f_m(\alpha) < \tilde{\rho}_0(\alpha) < f_r(\alpha)$ for any $\alpha \in (0, 1)$ where $f_i(\alpha) = \alpha(1 - \alpha)\tilde{\varphi}_i / [\alpha + (1 - \alpha)\tilde{\delta}]^2$ with $i \in \{m, r\}$ it follows that $\tilde{\delta} / (1 + \tilde{\delta}) < \alpha_{max} < 1$ where $\tilde{\delta} / (1 + \tilde{\delta}) = \operatorname{argmax}_{\alpha \in (0, 1)} \{f_i(\alpha)\}$ and $\alpha_{max} = \operatorname{argmax}_{\alpha \in (0, 1)} \{\tilde{\rho}_0(\alpha)\}$. Then, we have that:

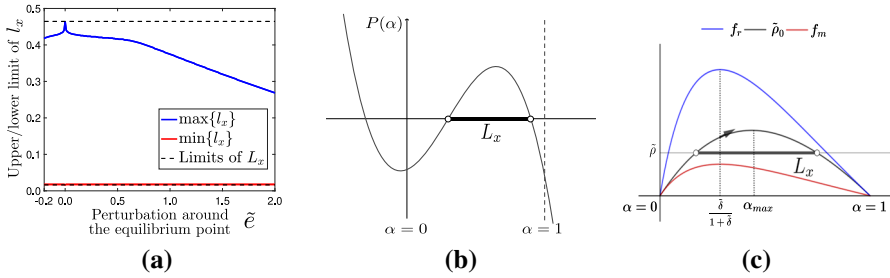


Fig. 6 Parametric dependence and functional conditions associated with stability behavior. **a** Dependence of $|L_x|$ according to initial state $Z_0 = (u^* + \tilde{e}, v^* + \tilde{e}, w^* + \tilde{e})$ for $e \in [-0.2, 2]$ and taking the parameter set $\psi = (0.7, 0.4, 1.0, 0.5, 0.1)$ on the system (8) into temporal range $[0, 1000]$. **b** Plot of the polynomial P whose coefficients take values in the set Γ and imply the existence of the maximal stability range L_x . **c** Plot of inequality $\tilde{\rho} < \tilde{\rho}_0(\alpha)$ for $\alpha \in (0, 1)$ where $f_i(\alpha) = \alpha(1 - \alpha)\tilde{\varphi}_i / [\alpha + (1 - \alpha)\tilde{\delta}]^2$ with $i \in \{m, r\}$. Here, the row on the $\tilde{\rho}_0$ curve represents the positive sign of the derivative of this function with respect to α at $\alpha = \tilde{\delta} / (1 + \tilde{\delta})$ equal to $(\tilde{\varphi}_r - \tilde{\varphi}_m) / 4\tilde{\delta}$

- i. As δ increases is obtained that $|L_x|$ tends to zero, due to that the limits of L_x , both lower and upper, collapse to value one according to an increasing trend, even more, the energy allocation strategies contained into L_x favors to reproduction (see Fig. 7(a)).
- ii. As $\tilde{\varphi}_r$ increases, $|L_x|$ also increases as a consequence of the increase of the upper limit of L_x , whose length is not diminished by the increase in its lower limit. In addition, the energy allocation strategies contained in L_x favor to reproduction (see Fig. 7(b)). The contrary trend occurs when $\tilde{\varphi}_m$ increases, namely, maintenance is favored.
- iii. As $\tilde{\rho}$ increases, $|L_x|$ decreases due to the decrease of the upper limit of L_x which is not compensated by the decrease of its lower limit (see Fig. 7(c)). Here, the energy allocation strategies contained into L_x favors to maintenance.

3.2 Plastic case

3.2.1 Consumer-resource dynamics with a positive feedback allocation strategy

The temporal dynamic of the consumer-resource model (7) with a positive feedback allocation strategy is always unstable. Indeed, this investment strategy an unrestricted growth of the resource, and consequently, the consumer population will tend to extinction. Then, we can derive the following conclusion.

Proposition 3 *Let be $Y_\xi^+(t, Y_0)$ the solution of model (7) with a positive feedback allocation strategy such that at $t = 0$ is $Y_0 = (\alpha_0, u_0, v_0, w_0) \in [0, 1] \times \mathbb{R}_+^3$. Then,*

$$\lim_{t \rightarrow +\infty} Y_\xi^+(t, Y_0) = (1, +\infty, 0, 0)$$

is obtained.

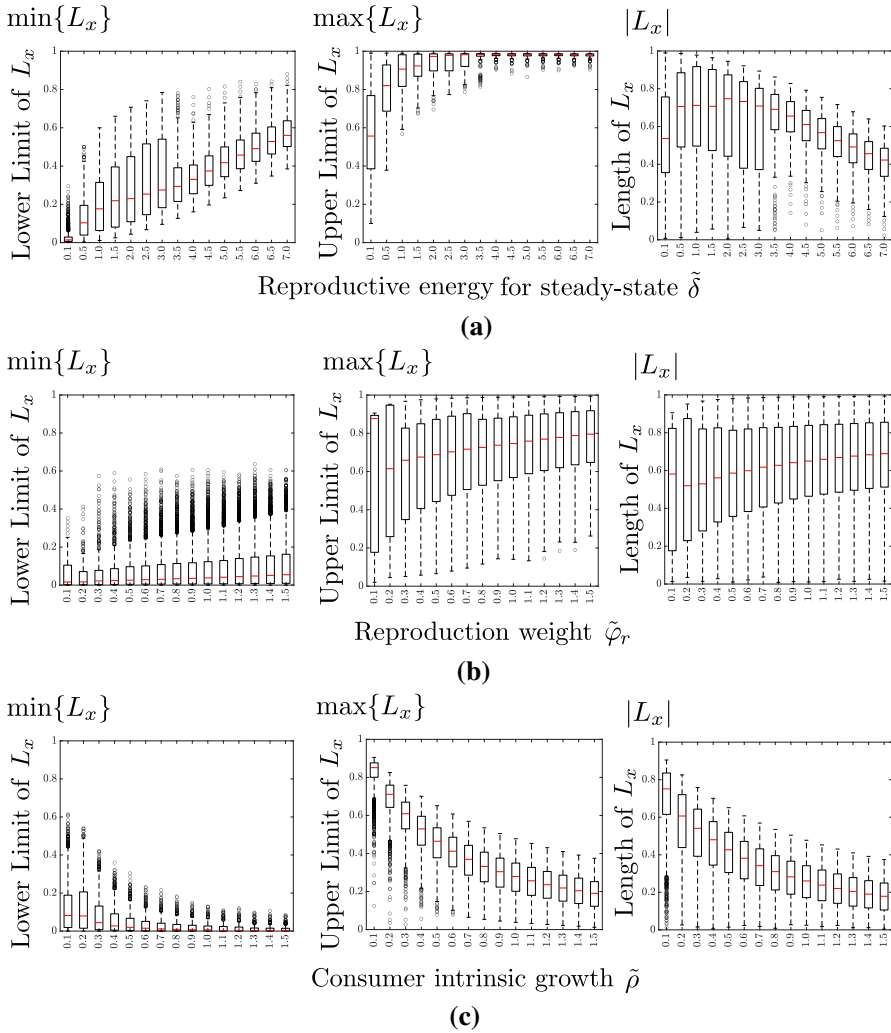


Fig. 7 Box plots of the lower limit, upper limit, and length of the maximal stability range L_x according to sets: **a** $(0, 1)^2 \times \{0.1, 0.5, \dots, 7.0\} \times (0, 1) \cap \Gamma$, **b** $\{0.1, \dots, 1.5\} \times (0, 1)^3 \cap \Gamma$, and **c** $(0, 1)^3 \times \{0.1, \dots, 1.5\} \cap \Gamma$. Here, we take a homogeneous partition for these sets with step size $h = 0.05$. The horizontal line within the box represents the median of each set, and the points that lie outside of the whiskers are outliers

Proof From equation (6) and positive feedback allocation strategy, given $\varepsilon_0 > 0$ there exists an integer number $N > 0$ such that for any $n \geq N$ we have:

- i) $\Delta u(\tau_n) < 0$ if, and only if, $0 < \alpha(\tau_n) < \varepsilon_0$, or equivalently $\lim_{t \rightarrow +\infty} u(t) = \lim_{t \rightarrow +\infty} \alpha(t) = 0$.
- ii) $\Delta u(\tau_n) > 0$ if, and only if, $0 < 1 - \alpha(\tau_n) < \varepsilon_0$, or equivalently $\lim_{t \rightarrow +\infty} u(t) = +\infty$, and $\lim_{t \rightarrow +\infty} \alpha(t) = 1$.

From Proposition 1(a) we have that whether $\alpha \in \{0, 1\}$ then $Z_\psi(t, Z_0) \rightarrow (+\infty, \{+\infty, 0\}, 0)$ as $t \rightarrow +\infty$ due to the equilibrium point $(0, 0, 0)$ is unstable.

On the one hand, $\Delta u(\tau_n) < 0$ for any $n \geq N$ implies that $\lim_{n \rightarrow +\infty} u(s_n) = 0$ which is absurd. Assuming $\alpha = 0$ in the impulsive system (7) and solving for u , we obtained

$$u(s) = u(s_n) \exp \left\{ \int_{s_n}^s [1 - f(k)] dk \right\}, \quad s \in (s_n, \tau_n], \tag{14}$$

where $f(s) = \{v(s)/(1 + v(s))\}w(s)$ such that $v(s)$ at $s = s_n$ is $(1 - c)v(s_n)$. In addition, from $w(s) = w(s_n)e^{-\tilde{\rho}\tilde{\delta}(s-s_n)}$ it follows that $w(\tau_n) = w(s_n)e^{-\tilde{\rho}\tilde{\delta}\tau}$. Evaluating (14) at $s = \tau_n$, we have that

$$\Delta u(\tau_n) = u(s_n)(e^{l\tau(1-f_n)} - 1), \quad \text{where } f_n = \frac{1}{l\tau} \int_{s_n}^{\tau_n} f(s) ds.$$

Thus, the fulfillment of $\Delta u(\tau_n) < 0$ is equivalent to $f_n > 1$ for any $n \geq N$. However,

$$|f_n| < \frac{1}{l\tau} \int_{s_n}^{\tau_n} |f(s)| ds < \frac{w(s_n)}{l\tau} \int_{s_n}^{\tau_n} e^{-\tilde{\rho}\tilde{\delta}(k-s_n)} dk = \kappa \cdot e^{-\tilde{\rho}\tilde{\delta}s_n},$$

where $\kappa = w(0)(1 - e^{-\tilde{\rho}\tilde{\delta}l\tau})/\tilde{\rho}\tilde{\delta}l\tau$. Thus, $|f_n| \rightarrow 0$ as $n \rightarrow +\infty$. On the other hand, taking $\alpha = 1$ the analytic solution of impulsive system (7) is given by

$$\begin{cases} u(s) = u(s_n)e^{s-s_n}, \\ v(s) = (1 - c)v(s_n)e^{-\tilde{\varphi}_r(s-s_n)}, \\ w(s) = w(s_n)e^{\tilde{\rho}\left\{\frac{(1-c)v(s_n)}{\tilde{\varphi}_r}\right\}[1 - e^{-\tilde{\varphi}_r(s-s_n)}] - \tilde{\delta}(s-s_n)}, \end{cases}$$

for any $s \in (s_n, \tau_n]$. Evaluating at $s = \tau_n$ it is possible to relate the vector $(u, v, w)_{(s_{n+1})}$ with $(u, v, w)_{(s_n)}$. Thus, the stroboscopic map

$$\begin{cases} u(s_{n+1}) = u(s_n)e^\tau, \\ v(s_{n+1}) = (1 - c)v(s_n)e^{-\tilde{\varphi}_r\tau}, \\ w(s_{n+1}) = w(s_n)e^{\tilde{\rho}\left\{\frac{(1-c)v(s_n)}{\tilde{\varphi}_r}\right\}(1 - e^{-\tilde{\varphi}_r\tau}) - \tilde{\delta}\tau}, \end{cases}$$

is obtained. Therefore, in both cases it concluded that $u(s_n) \rightarrow +\infty$, $v(s_n) \rightarrow 0$, and $w(s_n) \rightarrow 0$ as $n \rightarrow +\infty$.

Finally, the stability case is impossible, namely, given $\varepsilon_0, \varepsilon_1 > 0$ there exists $N > 0$ such that $|\Delta u(\tau_n)| < \varepsilon_1$ if, and only if, $|\alpha(\tau_n^+) - \alpha(\tau_n)| = |G(z(\tau_n))| < \varepsilon_0$ for any $n \geq N$, or equivalently $\lim_{t \rightarrow +\infty} u(t) = u^*(\alpha_\infty) > 0$ and $\lim_{t \rightarrow +\infty} \alpha(t) = \alpha_\infty \in (0, 1)$. Indeed, from the previous analysis, it concludes that if there exists an integer number $n_1 \geq 0$ such that $\Delta u(\tau_{n_1}) < 0$ then also there exists an integer number $n_2 > n_1$ such that $\Delta u(\tau_{n_2}) > 0$. Consequently, $\alpha(\tau_{n_2}^+) = \alpha(\tau_{n_2}) + G(z(\tau_{n_2})) > \alpha(\tau_{n_2})$ and $\alpha(\tau_{n_1}) > \alpha(\tau_{n_1+1}) > \alpha(\tau_{n_1+2}) > \dots > \alpha(\tau_{n_1+N}) > \alpha(\tau_{n_2})$ are obtained (see Fig. 8). From item i) it follows that a decreasing sequence of energy allocation $\{\alpha(\tau_n)\}$ implies later the resource increase. This, in turn, generates that $\{\alpha(\tau_n)\}$ increases, which by item

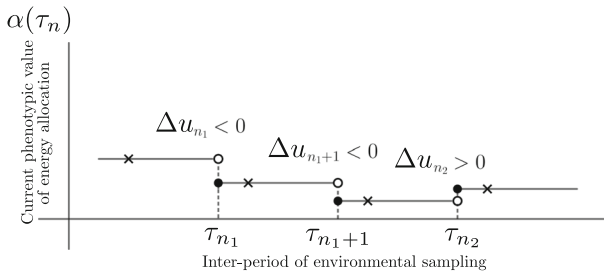


Fig. 8 Temporal dynamics of energy investment to reproduction according to the positive feedback allocation strategy. The symbol x correspond to energy allocation at $s \in \{s_{n_1}, s_{n_1+1}, s_{n_2}, s_{n_2+1}, \dots\}$ and $\Delta u_n = u(\tau_n) - u(s_n)$ with $\tau_n = s_n + l\tau$

ii) implies the resource increase. The energy allocation strategy according to positive feedback implies that $u(s)$ does not stabilize at a long-term equilibrium value. \square

3.2.2 Consumer-resource dynamics with a negative feedback allocation strategy

The consumption process restrains the growth of the resource more intensely when the energy allocation favors maintenance in contrast to reproduction. However, the trade-off between reproduction and survival implies that when the energy allocation towards maintenance increases, the per capita rate growth of consumers decreases, and consequently, also consumption decreases. Despite this, the negative feedback allocation strategy showed that the unstable pattern of the temporal dynamics of the consumer-resource model (7) is not the only potential outcome, as it is able to promote stable and oscillating behaviors depending on parameter values that are associated with the magnitude of the energy allocation change, moments of environmental sensibility and phenotype shift, and the fraction of maintenance phenotypic costs.

The analysis is carried out from numerical simulation of trajectories $\alpha(s)$ and $u(s)$ under the simplifying assumptions of stable and unstable patterns showed convergence at a fixed value ($\alpha_k = \alpha(\tau_k) > \delta_0$, $|u_k - u^*(\alpha_k)| < \epsilon_0$ and $|G(z(\tau_k))| < \delta_1$ where $u_k = \text{median}\{u(s) : s_k < s < s_{k+1}\}$ for k large enough), periodic behavior ($\alpha_k > \delta_0$, $|G(z(\tau_k))| \geq \delta_1$ and $|\Delta(|G(z(\tau_k))||)| < \delta_2$ for k large enough), and unrestricted growth of exponential type ($u(\tau_k) = \infty$ or $\alpha_k \leq \delta_0$ for k large enough). From these conditions, it is also possible to obtain quasi-periodic trajectories.

The procedure for finding the dynamic patterns of model (7) according to parameter combinations into the set $\{(U_0, \sigma_0), (\sigma_0, \theta), (\theta, U_0), (\tau, l), (U_0, c)\}$ is summarized in Procedure 2 (see appendix).

Firstly, the magnitude of the energy allocation change is dependent on three parameters: U_0 , σ_0 , and θ . At increasing values of U_0 , and as σ_0 and θ decrease, the temporal dynamics of the model (7) is predominantly stable and therefore converge to an equilibrium value in the long term (see Fig. 9, the region white). On the contrary, at decreasing values of U_0 , and as σ_0 and θ increase, the temporal dynamics of the model (7) is predominantly unstable. Here, a periodic behavior is obtained for the resource biomass and the energy allocation implying an oscillating persistence in the

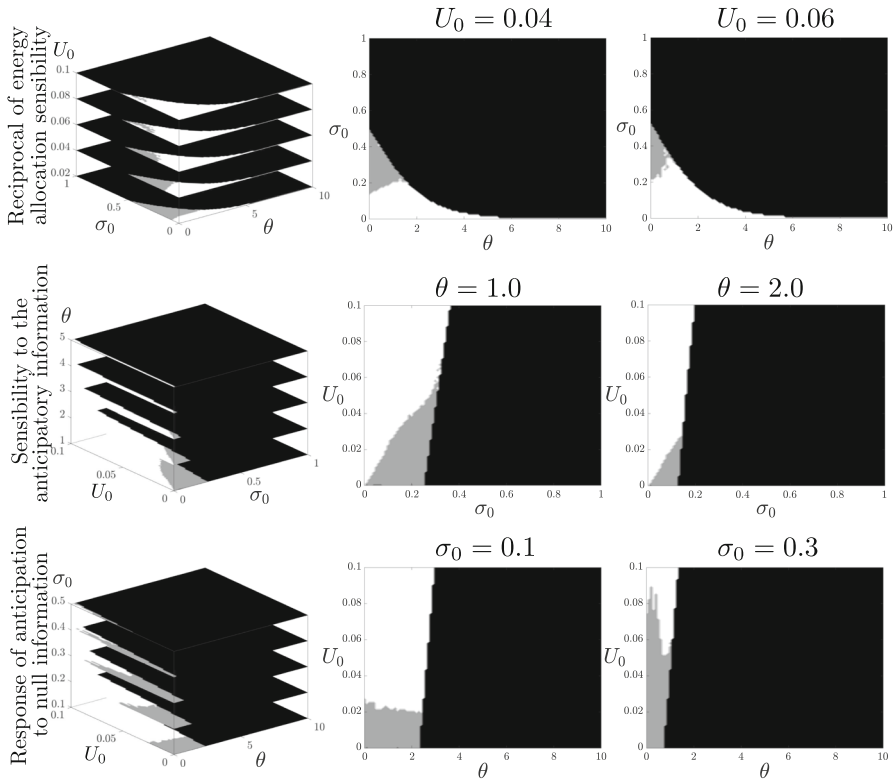


Fig. 9 Parameter combinations of the reciprocal of energy allocation sensibility U_0 , sensibility to the anticipatory information σ_0 , and the response of anticipation to null information θ , for which the temporal dynamics of model (7) is stable and converging to an equilibrium value (the region white), unstable either by an oscillating behavior (the region gray) or unrestricted growth of resource (the region black). The other parameters have default values according to Table 2 and initial condition $Y_0 = (0.5, 1, 1, 1)$ (color figure online)

consumer-resource dynamics (see Fig. 9, the region gray). Likewise, an extinction trend of the consumer population, and consequently, unrestricted resource growth is obtained from a monotonous increase or unbounded oscillations pattern (see Fig. 9, the region black). We conclude that the stable behavior is promoted to a greater extent by the variation of parameter U_0 in contrast to the variation of parameters σ_0 and θ .

Secondly, $l\tau$ is the time lag between environmental sensibility and plastic phenotype expression. Fig 10, reveals that there exists a positive constant C , which depending at least on U_0 , such that for $l\tau > C$ the temporal dynamics of model (7) is unstable having a periodic behavior. Contrary, when $l\tau < C$, the temporal dynamics can be stable converging to equilibrium value or unstable as a consequence of unrestricted growth of resource and consumer population extinction. A negative relation between l and τ indicates that whether the plastic phenotype expression promptly occurs subsequent to environmental information being obtained, the stable dynamic will predominate. However, if obtaining environmental information occurs more frequently, namely as

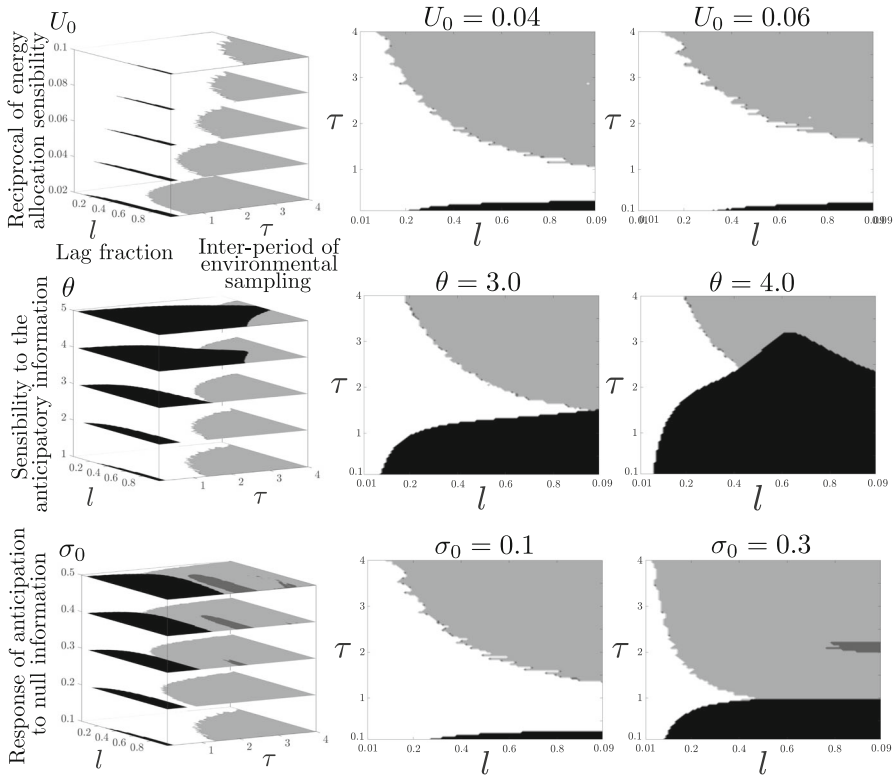


Fig. 10 Parameter combinations of inter-period of environmental sampling τ and lag fraction l according to initial condition $Y_0 = (0.5, 1, 1, 1)$ and (U_0, σ_0, θ) , for which the temporal dynamics of model (7) is stable and converging to an equilibrium value (the region white) or unstable either by an oscillating behavior (the region gray) or unrestricted growth of resource (the region black). Here, Top: $\sigma_0 = 0.1$ and $\theta = 1.0$, Center: $U_0 = 0.05$ and $\sigma_0 = 0.1$, and Bottom: $U_0 = 0.05$ and $\theta = 1.0$. The other parameters have default values according to Table 2 (color figure online)

τ^{-1} increases, but the plastic phenotypic expression occurs belatedly the dynamic will be unstable.

Thirdly, Fig 11(a) presents the combinations of U_0 and c for which temporal dynamics of model (7) is stable or unstable. There exists a wide region at which the consumer-resource dynamics cannot persist. Consequently, general maintenance of phenotypic costs will lead to the extinction of the consumer population. However, at low values of U_0 and c the consumer-resource dynamics persist showing an oscillating pattern either periodic or quasi-periodic (see Fig. 11(b)). Contrary, as U_0 increases but considering c , a small region emerges in which the stable behavior of temporal dynamics is guaranteed.

In conclusion, the temporal dynamics will be predominantly stable if the magnitude of the energy allocation change is not excessively large or if the time lag between sensibility environmental and plastic trait expression is short, assuming reduced plasticity

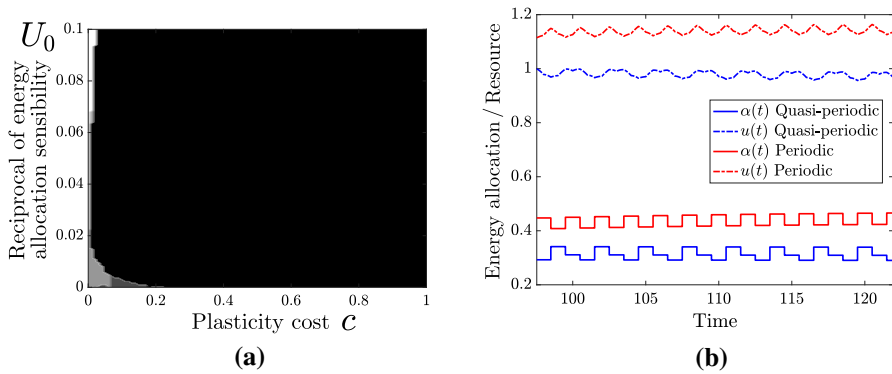


Fig. 11 (a) Parameter combinations of reciprocal of energy allocation sensibility U_0 and plasticity costs c according to initial condition $Y_0 = (0.5, 1, 1, 1)$, for which the temporal dynamics of model (7) is stable and converging to an equilibrium value (the region white) or unstable either by a periodic behavior (the region light grey), quasi-periodic behavior (the region black grey) or unrestricted growth of resource (the region black). (b) Periodic and quasi-periodic trajectories of resource and energy allocation taking the combinations $(0.033, 0.0047)$ and $(0.07, 0.004)$. The other parameters have default values according to Table 2 (color figure online)

costs. For this to occur, the parameters involved: $U_0, \sigma_0, \theta, l, \tau,$ and c will be restricted to specific subsets of its admissible sets.

3.2.3 Stability range

Let be $Y_\xi^-(t, Y_0)$ the solution of model (7) with a negative feedback allocation strategy such that at $t = 0$ is $Y_0 = (\alpha_0, u_0, v_0, w_0) \in [0, 1] \times \mathbb{R}_+^3$. As an extension of stability range (13), we define the set

$$\mathcal{L}_x = \left\{ \alpha_0 \in [0, 1] : \lim_{t \rightarrow +\infty} Y_\xi^-(t, Y_0) = (\alpha_\infty, P_1(\alpha_\infty)) \right\}, \tag{15}$$

where $\alpha_\infty := \lim_{t \rightarrow +\infty} \alpha(t, \alpha_0) \in (0, 1)$. This interval is a set of initial conditions of energy allocations for which the temporal dynamics of the model (7) is stable and whose trajectory converges to an equilibrium value. In the non-plastic case is assumed that $\alpha(t) = \alpha_0$ for any $t \geq 0$, whereas in the plastic case this value is only the initial allocation. In this sense, \mathcal{L}_x can contain energy allocation strategies that in l_x have no place. The procedure to obtain \mathcal{L}_x is similar to the procedure used to determine l_x and summarized in Procedure 3 (see appendix).

Fig 12, illustrates that the extension of the stability range l_x is possible. From Proposition 1 and Proposition 2, it follows that for energy allocation values near to limits of this range unstable dynamical patterns emerge. However, when the energy allocation is a plastic trait, a wide portion of these values leads to stable patterns. In the non-plastic case, each orbit converges to its respective stable point $P_1(\alpha)$ which clearly differ from each other (see Fig. 12(a)), whereas in the plastic case, the orbits

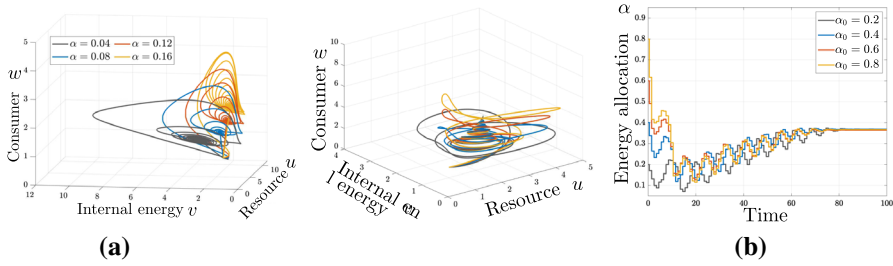


Fig. 12 Consumer-resource dynamics comparison of models (4) and (7) according to stability ranges. **(a)** Orbit of $Z_0 = (1, 1, 1)$ on the system (4) for different energy allocation values taken in the stability range $I_x \approx (0.0378, 0.183) \subseteq L_x = (0.0334, 0.2502)$. **(b)** Orbit of $Y_0 = (\alpha_0, 1, 1, 1)$ on the system (7) and energy allocation trajectory for different initial energy allocation values taken in the range $\mathcal{L}_x \approx [0.13, 1]$. These sets are obtained using Procedure 1 and Procedure 3, respectively. The parameters have default values according to Table 2 and assume a temporal limit $T = 100$

have a similar convergence trend in correspondence with a similar long-term energy allocation value, independently of the initial condition (see Fig. 12(b)).

In general, the stability range \mathcal{L}_x is not a continuum set. Indeed, a slight variation in the initial energy allocation selected into the set \mathcal{L}_x can imply temporal dynamics characterized by drastic changes, *i.e.*, from stable to unstable patterns. This is shown in Fig 13, which reveals that the continuity property is strengthened as U_0 increases and weakens at increasing values of σ_0 . Even more, \mathcal{L}_x is an empty set as σ_0 increases ($\sigma_0 \gtrsim 0.4$). This observation is consistent with the analysis carried out in the consumer-resource temporal dynamics section: the larger the set \mathcal{L}_x , the higher predomination of the stable dynamic pattern.

4 Discussion

In our article, we incorporated the energy allocation towards reproductive vs. maintenance on the consumer-resource interaction using a mechanistic approach. Our aim was to analyze how the effect of energy allocation strategies drives the directional variation of available resources on consumer-resource dynamics. We compared the temporal dynamics of two models, termed plastic and non-plastic, aiming to evaluate the stabilizing role of plastic energy allocation on consumer-resource dynamics. For both models, given by the systems (4) and (7), classical temporal dynamics are obtained. These dynamical patterns correspond to stable trajectories which converge in the long term to equilibrium values either in oscillatory or in an asymptotic fashion, or unstable trajectories with sustained periodic or quasi-periodic oscillations, or with unrestricted growth of exponential type.

Our attention was focused on the stable pattern of consumer-resource interaction. We found that stable trajectories are inherently related to the existence of an energy allocation range, termed stability range (see Fig. 6). The stability range is a physiological tolerance range where the allocation strategies belonging to this set allow the persistence and stability of the population of consumers over time (Gutiérrez et al. 2020). Additionally, our results reveal that the life-history strategy defined by the neg-

Table 2 The parameters and their default values for the system (7) with a positive feedback allocation strategy for visualizing the temporal dynamics and stability range \mathcal{L}_x taking initial condition $Y_0 = (\alpha_0, 1, 1, 1)$ for some $\alpha_0 \in [0, 1]$

Parameter	Default value	Fig. 9	Fig. 10	Fig. 11	Fig. 12	Fig. 13(a)	Fig. 13(b)	Fig. 13(c)
$\tilde{\varphi}_r, \tilde{\varphi}_m, \tilde{\delta}, \tilde{\rho}, \tilde{b}$	{0.6, 0.4, 0.1, 0.1, 1.0}				{0.91, 0.81, 0.11, 1.5, 1.0}			
U_0	Varying	{0.01,0.05,0.1}	Varying	0.1	Varying	0.1	0.1	0.1
σ_0	Varying	0.1	0.1	0.1	0.01	Varying	Varying	0.01
θ	Varying	1.0	1.0	1.0	1.0	1.0	1.0	Varying
τ	1.0	Varying	1.0	1.0	1.0	1.0	1.0	1.0
l	0.5	Varying	0.5	0.5	0.5	0.5	0.5	0.5
c	0.0	0.0	Varying	0.0	0.0	0.0	0.0	0.0

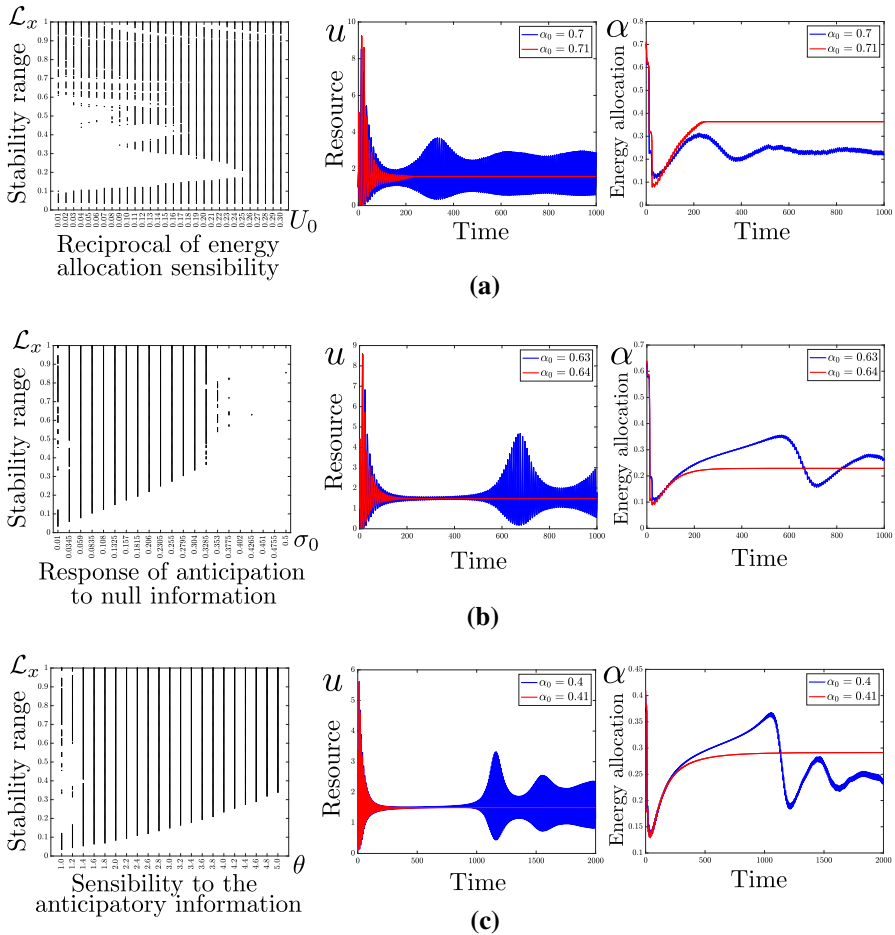


Fig. 13 Stability range \mathcal{L}_x according to the magnitude of energy allocation change parameters (Reciprocal of energy allocation sensibility U_0 , sensibility to the anticipatory information σ_0 , and the response of anticipation to null information θ) and temporal dynamics of resource and energy allocation for different initial conditions $Y_0 = (\alpha_0, 1, 1, 1)$. (a) \mathcal{L}_x vs. U_0 and temporal dynamics according to $U_0 = 0.01$, $\sigma_0 = 0.01$ and $\theta = 1.0$, (b) \mathcal{L}_x vs. σ_0 and temporal dynamics according to $U_0 = 0.1$, $\sigma_0 = 0.01$ and $\theta = 1.0$, and (c) \mathcal{L}_x vs. θ and temporal dynamics according to $U_0 = 0.1$, $\sigma_0 = 0.01$ and $\theta = 1.4$. These sets are obtained using Procedure 3 where is assumed a temporal limit $T \in \{1000, 2000\}$ and a homogeneous partition of the interval $[0, 1]$ with step size $h = 0.005$. The other parameters have default values according to Table 2

ative feedback between available resources and the energy investment in reproduction promotes the stability of the consumer-resource interaction. Both the magnitude at which the change in the energy allocation occurs and the time lag that takes to express the new phenotypic value of energy allocation are key elements that determine the stability of the dynamical pattern. Nonetheless, the phenotypic plasticity costs greatly limit the emerging stable pattern.

The plasticity degree is quantified by the slope of the reaction norm. From a linear reaction norm proposed, we obtained that the retrospective information has a greater influence in contrast to the anticipatory information in the determination of the stable pattern in the consumer-resource dynamics. This outcome is observed through the extension of the stability range l_x , denoted by \mathcal{L}_x (see Fig. 13). Here, the energy allocation sensibility to the net variation of the available resource, given by U_0^{-1} , has a key role (see Fig. 9). Excessive sensitivity may cause unstable patterns to appear, whereas a reduced sensitivity may not be sufficient to promote the stable pattern beyond what the stability range establishes due to the equivalence of systems (4) and (7). At these extremes, plasticity is not beneficial, even more, being very responsive to the net variation of the available resource can be detrimental (Chevin et al. 2013).

The calculation of the net variation of the available resource is carried out from the resource level at two instants, separated by time units. This time lag is the period devoted to the development of a particular phenotype. We found that the time lag which promotes the stable pattern results from the combination of sampling of the inducing environment at instants with a sufficiently long period (τ) and high predictive power of the selective environment associated with the period (l) (see Fig. 10) (Nijhout 2003). Despite our mathematical formulation does not consider a reliable cue (e.g., driven by temperature, rain, or photoperiod) in determining the inducing environment, our results capture the time-lag nature according to Nijhout (2003).

Plasticity costs are relevant in the expression of phenotypic plasticity (Fischer et al. 2009). Studies focused on quantifying the costs of plasticity have concluded these are low or absent (Van Kleunen and Fischer 2005; Van Buskirk and Steiner 2009). However, despite this, the low plasticity costs can drive populations toward extinction. Our results are consistent with this, which shows the energetic costs that demand the phenotypic plasticity although small, are significantly able to destabilize the temporal dynamics of the consumer population, leading even to extinction (see Fig. 11). According to Auld et al. 2010, plasticity costs are concentrated in two ways, the first being a consequence of the ability to be plastic, and the second results from expressing a suboptimal phenotype in a given environment. We only consider the first type of cost, evidenced through an energy payment due to the maintenance and use of sensory systems (DeWitt et al. 1998). On the other hand, the expression of a “wrong phenotype” in response to an inaccurate cue (Schlaepfer et al. 2002) was assumed to not carry any energetic cost. When this cost exists, the plasticity would be considered maladaptive (Ghalambor et al. 2007; Hendry 2015). This cost could be modulated by the similarity degree between phenotype $\alpha(s^+)$ and optimal phenotype $\alpha_{op}(s)$, previously established, in a given resource level $u(s)$ (Reed et al. 2010), so that the model (7) must incorporate

$$v(s^+) = \{1 - f(|\alpha(s^+) - \alpha_{op}(s)|)\}v(s)$$

at $s = \tau_n$, where $f : \mathbb{R}_0^+ \rightarrow [0, 1]$ is an increasing function such that $f(0) = 0$. Given our results, an additional decrease in organisms’ internal energy could promote the instability of the consumer-resource dynamic and even accentuate the extinction risk (see Fig. 11(a)). Future research may evaluate the dependence of the fraction of lag (l)

with respect to the plastic phenotype (α). This will allow analyzing how the accuracy of the environmental signal affects the prediction of future conditions, and its effects on the reduction of the difference between suboptimal and optimal phenotypes.

Our modeling approach does not focus on finding the optimal energy allocation patterns underlying the consumer-resource dynamics, which certainly represents a challenge that prompts future research. Motivated by Fischer et al. (2009) and Gutiérrez et al. (2020), we analyzed temporal dynamics of consumer-resource interaction in the function of the energy allocation to reproduction vs. maintenance as a plastic trait according to the available resource. However, this is not the only framework from which the impact of plastic energy allocation on population dynamics could be analyzed. From the traditional approach (Ziółko and Kozłowski 1983; Kozłowski and Wiegert 1986; Engen and Saether 1994), which has been recently extended (Johansson et al. 2018), the energy allocation toward reproduction can depend on the body size of organisms instead of the available resource. By exploring each allocation program obtained by Johansson et al. (2018), at the population level, which temporal dynamical patterns can we expect?

We think that an approximation to answer such a question must consider an extension of the trade-off between two traits given by the Y-model, with values determined by the proportion of energetic resources allocated to each (Van Noordwijk and de Jong 1986; Ng'oma et al. 2017). The individual life-history framework states that both reproduction and survival are depending on the age-specific, without considering the influence that body size can have on these functions (Steiner et al. 2014; Keyfitz and Caswell 2005). Indeed, the interconnections between reproduction and survival are obtained from underlying mechanisms relatives to the energetic costs and consumption efficiency, which usually are formulated in terms of the body size and described by allometric laws (Blueweiss et al. 1978; Kooijman 2000). In age-structured populations, the dynamic patterns are understood from two macroscopic parameters, the net reproductive rate \mathcal{R}_0 given by the accumulative age-specific birthrate adjusted by survivorship, and the average age at which an individual reproduces T_c (Steiner et al. 2014). Thus, we propose an age-specific birthrate composed of both the reproductive effort and the degree of parental care. The first term could be defined by the product between allocation to reproduction and the organism's internal energy, and the second term by the product between complementary allocation to foraging (dependent on the complementary allocation to both reproduction and growing) and the organism's internal energy (see Fig. 14). Consequently, the remaining energy is destined for growing and foraging.

Importantly, the body size may be associated with the developmental stages, where its incorporation in an age-structured dynamic can induce a stage-age structured dynamic, in which survival and reproduction vary according to size and age (Steiner et al. 2014; Keyfitz and Caswell 2005). On the one hand, the age variable provides an understanding at the individual level in relation to the environment, and on the other hand, the size variable allows scaling at the population level from the grouping of individuals by age. According to our approach, body size is a plastic trait, due to energy allocation, where individuals of the same age may differ in size. Thus, the stage-age structured models provide an adequate framework for which to address this future challenge.

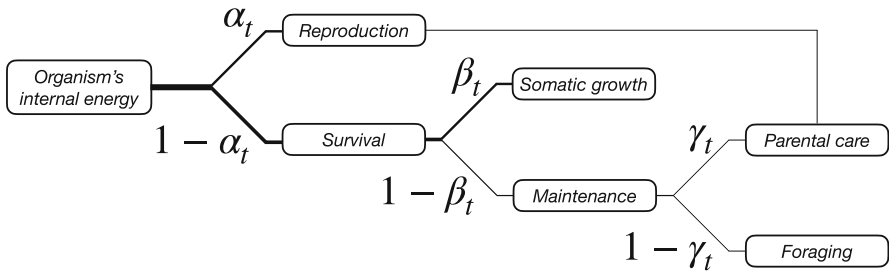


Fig. 14 Energy allocation toward reproduction vs. survival with secondary and tertiary trade-offs between (i) somatic growth vs. maintenance, and (ii) parental care vs. foraging, respectively. Here, $\alpha_t + (1 - \alpha_t)(1 - \beta_t)\gamma_t$ is the proportion of organism's internal energy allocated to reproduction, $(1 - \alpha_t)\beta_t$ is the proportion of organism's internal energy allocated to somatic growth, and $(1 - \alpha_t)(1 - \beta_t)(1 - \gamma_t)$ is the proportion of organism's internal energy allocated to foraging at age-specific $t = 0, 1, 2, \dots, T$ with $0 \leq \alpha_t, \beta_t, \gamma_t \leq 1$. The thickness of each connection line represents the value of the energy allocation

Acknowledgements Rodrigo Gutiérrez would like to thank Vicerrectoría de Investigación y Postgrado at Universidad Católica del Maule, Chile. This paper is part of Rodrigo Gutiérrez Ph.D. thesis in the Program Doctorado en Modelamiento Matemático Aplicado at Universidad Católica del Maule, Chile. The authors also wish to thank the referee for a careful reading of the manuscript, and for useful comments and suggestions that markedly improved their paper.

Author Contributions All authors contributed to the study conception and design. Material preparation and analysis of the mathematical model, both analytic and numeric, were performed by Rodrigo Gutiérrez. The first draft of the manuscript was written by Rodrigo Gutiérrez and all authors commented on previous versions of the manuscript. All authors read and approved the final manuscript.

Declarations

Conflict of interest The authors declare that they have no conflict of interest.

A Coefficients of functions $F_1, G_1,$ and $H_1.$

Let be $F_1(X, Y, Z) = a_{200}X^2 + a_{020}Y^2 + a_{110}XY + a_{101}XZ + a_{011}YZ + a_{210}X^2Y + a_{201}X^2Z + a_{111}XYZ + a_{120}XY^2 + a_{021}Y^2Z + a_{102}XZ^2 + a_{012}YZ^2 + a_{300}X^3,$
 $G_1(X, Y, Z) = b_{200}X^2 + b_{020}Y^2 + b_{002}Z^2 + b_{110}XY + b_{101}XZ + b_{011}YZ + b_{210}X^2Y + b_{201}X^2Z + b_{111}XYZ + b_{120}XY^2 + b_{021}Y^2Z + b_{102}XZ^2 + b_{012}YZ^2 + b_{300}X^3,$ and
 $H_1(X, Y, Z) = c_{200}X^2 + c_{020}Y^2 + c_{110}XY + c_{101}XZ + c_{011}YZ + c_{210}X^2Y + c_{201}X^2Z + c_{111}XYZ + c_{120}XY^2 + c_{021}Y^2Z + c_{102}XZ^2 + c_{012}YZ^2 + c_{300}X^3$ where

$$a_{200} = \frac{(1 - \alpha)^3 \tilde{\varphi} \tilde{\delta}^3 [2\alpha + (1 - \alpha)\tilde{\varphi} \tilde{\delta}]}{\alpha^2 + (1 - \alpha)\alpha \tilde{\delta} + (1 - \alpha)^2 \tilde{\varphi} \tilde{\delta}^2},$$

$$a_{020} = \frac{(1 - \alpha)^3 \tilde{b}^2 \tilde{\delta} [\alpha + (1 - \alpha)\tilde{\delta}]}{(1 - \alpha)^2 \tilde{\varphi} \tilde{\delta}^2 + \alpha [\alpha + (1 - \alpha)\tilde{\delta}]},$$

$$a_{110} = \frac{(1 - \alpha)^3 \alpha \tilde{\varphi} \tilde{b} \tilde{\delta}^2}{\alpha^2 + (1 - \alpha)\alpha \tilde{\delta} + (1 - \alpha)^2 \tilde{\varphi} \tilde{\delta}^2},$$

$$a_{101} = \frac{(1 - \alpha)^2 \tilde{\varphi} \tilde{b} (\alpha(-1 + \tilde{\delta}) - \tilde{\delta}) \tilde{\delta}^2 (-3\alpha + (-1 + \alpha)\tilde{\varphi} \tilde{\delta})}{\sqrt{\alpha + (1 - \alpha)\tilde{\delta} (\alpha^2 + (1 - \alpha)\alpha \tilde{\delta} + (1 - \alpha)^2 \tilde{\varphi} \tilde{\delta}^2)}},$$

$$\begin{aligned}
 a_{011} &= \frac{(1-\alpha)\tilde{b}^2(\alpha^3 + (1-\alpha)\alpha^2(2+\tilde{\varphi})\tilde{\delta} + (1-\alpha)^2\alpha\tilde{\delta}^2 - (1-\alpha)^3\tilde{\varphi}\tilde{\delta}^3)}{\sqrt{\alpha + (1-\alpha)\tilde{\delta}(\alpha^2 + (1-\alpha)\alpha\tilde{\delta} + (1-\alpha)^2\tilde{\varphi}\tilde{\delta}^2)}}, \\
 a_{210} &= -\frac{(1-\alpha)^3\alpha^2\tilde{b}\tilde{\delta}^2(-\alpha^2 - 2(1-\alpha)\alpha\tilde{\delta} + (1-\alpha)^2(-1+\tilde{\varphi})\tilde{\delta}^2)}{[\alpha + (1-\alpha)\tilde{\delta}][(1-\alpha)^2\tilde{\varphi}\tilde{\delta}^2 + \alpha[\alpha + (1-\alpha)\tilde{\delta}]]}, \\
 a_{201} &= -\frac{\alpha^2\tilde{\varphi}\tilde{b}(\tilde{\delta} - \alpha\tilde{\delta})^3(\tilde{\delta} - \alpha(1+\tilde{\delta}))}{\sqrt{\alpha + (1-\alpha)\tilde{\delta}((1-\alpha)^2\tilde{\varphi}\tilde{\delta}^2 + \alpha[\alpha + (1-\alpha)\tilde{\delta}])}}, \\
 a_{111} &= \frac{(1-\alpha)^2\alpha\tilde{b}^2\tilde{\delta}(\alpha^3 + 2(1-\alpha)\alpha^2\tilde{\delta} - (1-\alpha)^2\alpha(-1+\tilde{\varphi})\tilde{\delta}^2 + (1-\alpha)^3\tilde{\varphi}\tilde{\delta}^3)}{\sqrt{\alpha + (1-\alpha)\tilde{\delta}(\alpha^2 + (1-\alpha)\alpha\tilde{\delta} + (1-\alpha)^2\tilde{\varphi}\tilde{\delta}^2)}}, \\
 a_{120} &= -\frac{(1-\alpha)^4\alpha\tilde{b}^2\tilde{\delta}^2[\alpha + (1-\alpha)\tilde{\delta}]}{(1-\alpha)^2\tilde{\varphi}\tilde{\delta}^2 + \alpha[\alpha + (1-\alpha)\tilde{\delta}]}, \\
 a_{021} &= -\frac{\alpha(\tilde{b} - \alpha\tilde{b})^3\tilde{\delta}[\alpha + (1-\alpha)\tilde{\delta}]^{3/2}}{(1-\alpha)^2\tilde{\varphi}\tilde{\delta}^2 + \alpha[\alpha + (1-\alpha)\tilde{\delta}]}, \\
 a_{102} &= -\frac{\alpha^2\tilde{\varphi}\tilde{b}(\tilde{\delta} - \alpha\tilde{\delta})^3(\tilde{\delta} - \alpha(1+\tilde{\delta}))}{\sqrt{\alpha + (1-\alpha)\tilde{\delta}((1-\alpha)^2\tilde{\varphi}\tilde{\delta}^2 + \alpha[\alpha + (1-\alpha)\tilde{\delta}])}}, \\
 a_{012} &= \frac{(1-\alpha)^4\alpha\tilde{\varphi}\tilde{b}^3\tilde{\delta}^3}{(1-\alpha)^2\tilde{\varphi}\tilde{\delta}^2 + \alpha[\alpha + (1-\alpha)\tilde{\delta}]}, \\
 a_{300} &= \frac{\alpha^3\tilde{\varphi}(1-\alpha)^4\tilde{\delta}^4}{[\alpha + (1-\alpha)\tilde{\delta}][(1-\alpha)^2\tilde{\varphi}\tilde{\delta}^2 + \alpha[\alpha + (1-\alpha)\tilde{\delta}]]}, \\
 b_{200} &= \frac{(1-\alpha)\alpha^2\tilde{\varphi}\tilde{\delta}^2(\alpha^2 - 2(-1+\alpha)\alpha\tilde{\delta} + (1-\alpha)^2(1+2\tilde{\varphi})\tilde{\delta}^2)}{\tilde{b}[\alpha + (1-\alpha)\tilde{\delta}][(1-\alpha)^2\tilde{\varphi}\tilde{\delta}^2 + \alpha[\alpha + (1-\alpha)\tilde{\delta}]]}, \\
 b_{020} &= \frac{(1-\alpha)^2\alpha\tilde{b}\tilde{\delta}[\alpha + (1-\alpha)\tilde{\delta}]}{(1-\alpha)^2\tilde{\varphi}\tilde{\delta}^2 + \alpha[\alpha + (1-\alpha)\tilde{\delta}]}, \\
 b_{002} &= -\alpha\tilde{\varphi}\tilde{b}\tilde{\delta}, \\
 b_{110} &= \frac{(1-\alpha)^4\alpha\tilde{\varphi}^2\tilde{\delta}^4}{-\alpha^3 + 2(-1+\alpha)\alpha^2\tilde{\delta} - (1-\alpha)^2\alpha(1+\tilde{\varphi})\tilde{\delta}^2 - (1-\alpha)^3\tilde{\varphi}\tilde{\delta}^3}, \\
 b_{101} &= \frac{\alpha\tilde{\varphi}\tilde{\delta}(\alpha^3 - 2(-1+\alpha)\alpha^2\tilde{\delta} + (1-\alpha)^2\alpha(1+2\tilde{\varphi})\tilde{\delta}^2 - (1-\alpha)^3\tilde{\varphi}\tilde{\delta}^3)}{\sqrt{\alpha + (1-\alpha)\tilde{\delta}((1-\alpha)^2\tilde{\varphi}\tilde{\delta}^2 + \alpha[\alpha + (1-\alpha)\tilde{\delta}])}}, \\
 b_{011} &= \frac{\alpha\tilde{b}(\alpha^3 - 2(-1+\alpha)\alpha^2\tilde{\delta} - (1-\alpha)^2\alpha(-1+\tilde{\varphi})\tilde{\delta}^2 - (1-\alpha)^3\tilde{\varphi}(1+\tilde{\varphi})\tilde{\delta}^3)}{\sqrt{\alpha + (1-\alpha)\tilde{\delta}(\alpha^2 + (1-\alpha)\alpha\tilde{\delta} + (1-\alpha)^2\tilde{\varphi}\tilde{\delta}^2)}}, \\
 b_{210} &= \frac{(1-\alpha)^2\alpha^2\tilde{\delta}^2((1-\alpha)^4\tilde{\varphi}^2\tilde{\delta}^4 + \alpha[\alpha + (1-\alpha)\tilde{\delta}]^3)}{[\alpha + (1-\alpha)\tilde{\delta}]^2((1-\alpha)^2\tilde{\varphi}\tilde{\delta}^2 + \alpha[\alpha + (1-\alpha)\tilde{\delta}])}, \\
 b_{201} &= -\frac{(1-\alpha)^2\alpha^3\tilde{\varphi}\tilde{\delta}^3(\alpha^2 - 2(-1+\alpha)\alpha\tilde{\delta} + (1-\alpha)^2(1+2\tilde{\varphi})\tilde{\delta}^2)}{[\alpha + (1-\alpha)\tilde{\delta}]^{3/2}((1-\alpha)^2\tilde{\varphi}\tilde{\delta}^2 + \alpha[\alpha + (1-\alpha)\tilde{\delta}])}, \\
 b_{111} &= \frac{(1-\alpha)\alpha^2\tilde{b}\tilde{\delta}(\alpha[\alpha + (1-\alpha)\tilde{\delta}]^3 + \tilde{\varphi}(\tilde{\delta} - \alpha\tilde{\delta})^2(\alpha^2 - 2(-1+\alpha)\alpha\tilde{\delta} + (1-\alpha)^2(1+2\tilde{\varphi})\tilde{\delta}^2))}{[\alpha + (1-\alpha)\tilde{\delta}]^{3/2}((1-\alpha)^2\tilde{\varphi}\tilde{\delta}^2 + \alpha[\alpha + (1-\alpha)\tilde{\delta}])}, \\
 b_{120} &= -\frac{(1-\alpha)^3\alpha^2\tilde{b}\tilde{\delta}^2[\alpha + (1-\alpha)\tilde{\delta}]}{(1-\alpha)^2\tilde{\varphi}\tilde{\delta}^2 + \alpha[\alpha + (1-\alpha)\tilde{\delta}]}, \\
 b_{021} &= -\frac{(1-\alpha)^2\alpha^2\tilde{b}^2\tilde{\delta}[\alpha + (1-\alpha)\tilde{\delta}]^{3/2}}{(1-\alpha)^2\tilde{\varphi}\tilde{\delta}^2 + \alpha[\alpha + (1-\alpha)\tilde{\delta}]},
 \end{aligned}$$

$$\begin{aligned}
 b_{102} &= -\frac{(1-\alpha)\alpha^3\tilde{\varphi}\tilde{b}\tilde{\delta}^2(\alpha^2-2(-1+\alpha)\alpha\tilde{\delta}+(1-\alpha)^2(1+\tilde{\varphi})\tilde{\delta}^2)}{[\alpha+(1-\alpha)\tilde{\delta}]\left((1-\alpha)^2\tilde{\varphi}\tilde{\delta}^2+\alpha[\alpha+(1-\alpha)\tilde{\delta}]\right)}, \\
 b_{012} &= \frac{(1-\alpha)^2\alpha^2\tilde{\varphi}\tilde{b}^2\tilde{\delta}^2(\alpha^2-2(-1+\alpha)\alpha\tilde{\delta}+(1-\alpha)^2(1+\tilde{\varphi})\tilde{\delta}^2)}{[\alpha+(1-\alpha)\tilde{\delta}]\left((1-\alpha)^2\tilde{\varphi}\tilde{\delta}^2+\alpha[\alpha+(1-\alpha)\tilde{\delta}]\right)}, \\
 b_{300} &= -\frac{(1-\alpha)^5\alpha^3\tilde{\varphi}^2\tilde{\delta}^6}{\tilde{b}[\alpha+(1-\alpha)\tilde{\delta}]^2\left((1-\alpha)^2\tilde{\varphi}\tilde{\delta}^2+\alpha[\alpha+(1-\alpha)\tilde{\delta}]\right)}, \\
 c_{200} &= \frac{\alpha\tilde{\varphi}(\alpha+(-1+\alpha)\tilde{\delta})(\tilde{\delta}-\alpha\tilde{\delta})^3}{\tilde{b}\sqrt{\alpha+\tilde{\delta}-\alpha\tilde{\delta}}\left((1-\alpha)^2\tilde{\varphi}\tilde{\delta}^2+\alpha[\alpha+(1-\alpha)\tilde{\delta}]\right)}, \\
 c_{020} &= -\frac{(1-\alpha)^4\tilde{b}\tilde{\delta}^2\sqrt{\alpha+(1-\alpha)\tilde{\delta}}}{(1-\alpha)^2\tilde{\varphi}\tilde{\delta}^2+\alpha[\alpha+(1-\alpha)\tilde{\delta}]}, \\
 c_{110} &= \frac{(1-\alpha)^2\tilde{\delta}\left((1-\alpha)^3\tilde{\varphi}\tilde{\delta}^3+\alpha[\alpha+(1-\alpha)\tilde{\delta}]\right)^2}{\sqrt{\alpha+(1-\alpha)\tilde{\delta}}\left((1-\alpha)^2\tilde{\varphi}\tilde{\delta}^2+\alpha[\alpha+(1-\alpha)\tilde{\delta}]\right)}, \\
 c_{101} &= \frac{(1-\alpha)^2\alpha\tilde{\varphi}\tilde{\delta}^2(\alpha+2(-1+\alpha)\tilde{\delta})}{\alpha^2+(1-\alpha)\alpha\tilde{\delta}+(1-\alpha)^2\tilde{\varphi}\tilde{\delta}^2}, \\
 c_{011} &= -\frac{(1-\alpha)\tilde{b}(-\alpha^3+(-1+\alpha)\alpha^2\tilde{\delta}-2(1-\alpha)^3\tilde{\varphi}\tilde{\delta}^3)}{\alpha^2+(1-\alpha)\alpha\tilde{\delta}+(1-\alpha)^2\tilde{\varphi}\tilde{\delta}^2}, \\
 c_{210} &= \frac{(1-\alpha)^4\alpha^2\tilde{\delta}^3(-\alpha^2-2(1-\alpha)\alpha\tilde{\delta}+(1-\alpha)^2(-1+\tilde{\varphi})\tilde{\delta}^2)}{[\alpha+(1-\alpha)\tilde{\delta}]^{3/2}\left((1-\alpha)^2\tilde{\varphi}\tilde{\delta}^2+\alpha[\alpha+(1-\alpha)\tilde{\delta}]\right)}, \\
 c_{201} &= \frac{\alpha^2\tilde{\varphi}(\tilde{\delta}-\alpha\tilde{\delta})^4(\tilde{\delta}-\alpha(1+\tilde{\delta}))}{[\alpha+(1-\alpha)\tilde{\delta}]\left((1-\alpha)^2\tilde{\varphi}\tilde{\delta}^2+\alpha[\alpha+(1-\alpha)\tilde{\delta}]\right)}, \\
 c_{111} &= -\frac{(1-\alpha)^3\alpha\tilde{b}\tilde{\delta}^2(-\alpha^3+2(-1+\alpha)\alpha^2\tilde{\delta}+(1-\alpha)^2\alpha(-1+\tilde{\varphi})\tilde{\delta}^2-(1-\alpha)^3\tilde{\varphi}\tilde{\delta}^3)}{-\alpha^3+2(-1+\alpha)\alpha^2\tilde{\delta}-(1-\alpha)^2\alpha(1+\tilde{\varphi})\tilde{\delta}^2-(1-\alpha)^3\tilde{\varphi}\tilde{\delta}^3}, \\
 c_{120} &= \frac{(1-\alpha)^5\alpha\tilde{b}\tilde{\delta}^3\sqrt{\alpha+(1-\alpha)\tilde{\delta}}}{(1-\alpha)^2\tilde{\varphi}\tilde{\delta}^2+\alpha[\alpha+(1-\alpha)\tilde{\delta}]}, \\
 c_{021} &= \frac{(1-\alpha)^4\alpha\tilde{b}^2\tilde{\delta}^2[\alpha+(1-\alpha)\tilde{\delta}]}{(1-\alpha)^2\tilde{\varphi}\tilde{\delta}^2+\alpha[\alpha+(1-\alpha)\tilde{\delta}]}, \\
 c_{102} &= \frac{(1-a)^4\alpha^2\tilde{\varphi}\tilde{b}\tilde{\delta}^4}{\sqrt{\alpha+\tilde{\delta}-\alpha\tilde{\delta}}(\alpha^2+(1-\alpha)\alpha\tilde{\delta}+(1-\alpha)^2\tilde{\varphi}\tilde{\delta}^2)}, \\
 c_{012} &= -\frac{(1-\alpha)^5\alpha\tilde{\varphi}\tilde{b}^2\tilde{\delta}^4}{\sqrt{\alpha+(1-\alpha)\tilde{\delta}}(\alpha^2+(1-\alpha)\alpha\tilde{\delta}+(1-\alpha)^2\tilde{\varphi}\tilde{\delta}^2)}, \\
 c_{300} &= -\frac{(1-\alpha)^5\alpha^3\tilde{\varphi}\tilde{\delta}^5}{\tilde{b}[\alpha+(1-\alpha)\tilde{\delta}]^{3/2}\left((1-\alpha)^2\tilde{\varphi}\tilde{\delta}^2+\alpha[\alpha+(1-\alpha)\tilde{\delta}]\right)},
 \end{aligned}$$

with $\tilde{\varphi} = \tilde{\varphi}_r\alpha + \tilde{\varphi}_m(1-\alpha)$.

B Coefficients associated to the value \mathcal{V}

$$\begin{aligned}
 a_0 &= -2\tilde{\delta}^8\tilde{\varphi}_m, a_1 = -2\tilde{\delta}^7(-1+(-1+15\tilde{\delta})\tilde{\varphi}_m-\tilde{\delta}\tilde{\varphi}_r), a_2 = -\tilde{\delta}^6(5+\tilde{\delta}^2(210\tilde{\varphi}_m+3\tilde{\varphi}_m^3+2\tilde{\varphi}_m^4-28\tilde{\varphi}_r)-2\tilde{\delta}(13+12\tilde{\varphi}_m+\tilde{\varphi}_m^2-\tilde{\varphi}_r)), \\
 a_3 &= \tilde{\delta}^5(-4+2\tilde{\delta}(26-5\tilde{\varphi}_m+\tilde{\varphi}_m^2)-\tilde{\delta}^2(156+27\tilde{\varphi}_m^2+5\tilde{\varphi}_m^3+\tilde{\varphi}_m(134-4\tilde{\varphi}_r)-22\tilde{\varphi}_r)+\tilde{\delta}^3(910\tilde{\varphi}_m+28\tilde{\varphi}_m^4+\tilde{\varphi}_m^3(39-8\tilde{\varphi}_r)-182\tilde{\varphi}_r-9\tilde{\varphi}_m^2\tilde{\varphi}_r)).
 \end{aligned}$$

$$\begin{aligned}
 a_4 = & -\delta^4(1 + \delta(-17 + 9\bar{\varphi}_m) + \delta^2(21\bar{\varphi}_m^2 + 2\bar{\varphi}_m^3 + 10(25 + \bar{\varphi}_r) - 4\bar{\varphi}_m(31 + \bar{\varphi}_r)) + \delta^3(-52\bar{\varphi}_m^3 + 8\bar{\varphi}_m^4 + \bar{\varphi}_m^2(-167 + 15\bar{\varphi}_r) + \\
 & \bar{\varphi}_m(-464 + 50\bar{\varphi}_r) - 2(286 - 56\bar{\varphi}_r + \bar{\varphi}_r^2)) + \delta^4(182\bar{\varphi}_m^4 - 728\bar{\varphi}_r + 12\bar{\varphi}_m^2(-9 + \bar{\varphi}_r)\bar{\varphi}_r - 26\bar{\varphi}_m^3(-9 + 4\bar{\varphi}_r) + 3\bar{\varphi}_m(910 + 3\bar{\varphi}_r^2)), \\
 a_5 = & \delta^4(-23 - 4\bar{\varphi}_m + \delta(19 + 123\bar{\varphi}_m + 10\bar{\varphi}_m^2 - 9\bar{\varphi}_r) - 2\delta^2(-370 + 3\bar{\varphi}_m^3 + 4\bar{\varphi}_m^4 - 57\bar{\varphi}_r - \bar{\varphi}_r^2 + \bar{\varphi}_m^2(-49 + 3\bar{\varphi}_r) + \bar{\varphi}_m(338 + 19\bar{\varphi}_r)) + \\
 & \delta^3(-1430 + 88\bar{\varphi}_m^4 + 352\bar{\varphi}_r - 23\bar{\varphi}_r^2 - 2\bar{\varphi}_m^3(125 + 16\bar{\varphi}_r) + 3\bar{\varphi}_m^2(-209 + 47\bar{\varphi}_r) + \bar{\varphi}_m(-1122 + 284\bar{\varphi}_r - 15\bar{\varphi}_r^2)) + \delta^4(728\bar{\varphi}_m^4 + 18\bar{\varphi}_m^3\bar{\varphi}_r(-33 + \\
 & 8\bar{\varphi}_r) - 78\bar{\varphi}_m^3(-11 + 8\bar{\varphi}_r) - \bar{\varphi}_r(2002 + 3\bar{\varphi}_r^2) + \bar{\varphi}_m(6006 + 99\bar{\varphi}_r^2 - 8\bar{\varphi}_r^3)), a_6 = -\delta^3(17 + \bar{\varphi}_m + \delta^2(284 + 106\bar{\varphi}_m^2 + 32\bar{\varphi}_m^3 + \bar{\varphi}_m(665 - \\
 & 20\bar{\varphi}_r) - 114\bar{\varphi}_r) - \delta(203 + 51\bar{\varphi}_m + 7\bar{\varphi}_m^2 - 4\bar{\varphi}_r) + \delta^3(1515 - 80\bar{\varphi}_m^4 + 562\bar{\varphi}_r + 17\bar{\varphi}_r^2 + 3\bar{\varphi}_m^2(91 + 8\bar{\varphi}_r) + 2\bar{\varphi}_m^3(-71 + 16\bar{\varphi}_r) + 2\bar{\varphi}_m(-1077 - \\
 & 79\bar{\varphi}_r + 3\bar{\varphi}_r^2) + \delta^4(-2574 + 440\bar{\varphi}_m^4 + 770\bar{\varphi}_r - 119\bar{\varphi}_r^2 + 5\bar{\varphi}_r^3 - 20\bar{\varphi}_m^3(37 + 16\bar{\varphi}_r) + \bar{\varphi}_m^2(-1595 + 609\bar{\varphi}_r + 48\bar{\varphi}_r^2) - 2\bar{\varphi}_m(1012 - 485\bar{\varphi}_r + \\
 & 63\bar{\varphi}_r^2) + \delta^5(2002\bar{\varphi}_m^4 + 396\bar{\varphi}_m^2\bar{\varphi}_r(-5 + 2\bar{\varphi}_r) - 143\bar{\varphi}_m^3(-15 + 16\bar{\varphi}_r) + 2\bar{\varphi}_r(-2002 - 15\bar{\varphi}_r^2 + \bar{\varphi}_r^3) - 11\bar{\varphi}_m(-910 - 45\bar{\varphi}_r^2 + 8\bar{\varphi}_r^3))), \\
 a_7 = & \delta^2(-3 - \delta^2(708 + 80\bar{\varphi}_m^2 + 12\bar{\varphi}_m^3 + \bar{\varphi}_m(233 - 14\bar{\varphi}_r) - 47\bar{\varphi}_r) + \delta(95 - 5\bar{\varphi}_m + \bar{\varphi}_m^2 - \bar{\varphi}_r) + \delta^3(864 + 256\bar{\varphi}_m^3 + \bar{\varphi}_m(1980 - 192\bar{\varphi}_r) + \bar{\varphi}_m^2(472 - \\
 & 96\bar{\varphi}_r) - 551\bar{\varphi}_r + 10\bar{\varphi}_r^2) - 2\delta^4(-1140 + 180\bar{\varphi}_m^4 + \bar{\varphi}_m^3(339 - 144\bar{\varphi}_r) - 796\bar{\varphi}_r - 31\bar{\varphi}_r^2 + \bar{\varphi}_r^3 + \bar{\varphi}_m(2238 + 194\bar{\varphi}_r + 15\bar{\varphi}_r^2) + \bar{\varphi}_m^2(-259 - 201\bar{\varphi}_r + \\
 & 24\bar{\varphi}_r^2) + \delta^6(4004\bar{\varphi}_m^4 + 165\bar{\varphi}_m^2\bar{\varphi}_r(-27 + 16\bar{\varphi}_r) - 143\bar{\varphi}_m^3(-27 + 40\bar{\varphi}_r) - 55\bar{\varphi}_m(-234 - 27\bar{\varphi}_r^2 + 8\bar{\varphi}_r^3) + \bar{\varphi}_r(-6006 - 135\bar{\varphi}_r^2 + 20\bar{\varphi}_r^3)) + \\
 & \delta^5(-3432 + 1320\bar{\varphi}_m^4 + 1254\bar{\varphi}_r - 366\bar{\varphi}_r^2 + 37\bar{\varphi}_r^3 - 15\bar{\varphi}_m^3(101 + 96\bar{\varphi}_r) + 3\bar{\varphi}_m^2(-968 + 537\bar{\varphi}_r + 144\bar{\varphi}_r^2) - \bar{\varphi}_m(2838 - 2220\bar{\varphi}_r + 483\bar{\varphi}_r^2 + 32\bar{\varphi}_r^3))), \\
 a_8 = & -\delta^2(-2 + 9\bar{\varphi}_m + \delta(237 + 23\bar{\varphi}_m^2 + 6\bar{\varphi}_r - 2\bar{\varphi}_m(37 + \bar{\varphi}_r)) - \delta^2(1398 + 84\bar{\varphi}_m^3 + \bar{\varphi}_m(571 - 146\bar{\varphi}_r) - 186\bar{\varphi}_r + 7\bar{\varphi}_r^2 - 4\bar{\varphi}_m^2(-85 + 9\bar{\varphi}_r)) + \\
 & \delta^3(1414 + 896\bar{\varphi}_m^3 - 1429\bar{\varphi}_r + 86\bar{\varphi}_r^2 - 168\bar{\varphi}_m^2(-7 + 4\bar{\varphi}_r) + \bar{\varphi}_m(3678 - 752\bar{\varphi}_r + 96\bar{\varphi}_r^2) - 2\delta^4(480\bar{\varphi}_m^4 + \bar{\varphi}_m^3(846 - 576\bar{\varphi}_r) + \bar{\varphi}_m^2(-365 - \\
 & 816\bar{\varphi}_r + 192\bar{\varphi}_r^2) + \bar{\varphi}_m(3192 + 324\bar{\varphi}_r + 186\bar{\varphi}_r^2 - 16\bar{\varphi}_r^3) - 2(651 + 721\bar{\varphi}_r + 33\bar{\varphi}_r^2 + 3\bar{\varphi}_r^3)) + 6\delta^6(1001\bar{\varphi}_m^4 - 858\bar{\varphi}_m^3(-1 + 2\bar{\varphi}_r) + 198\bar{\varphi}_m^2\bar{\varphi}_r(-6 + \\
 & 5\bar{\varphi}_r) - 55\bar{\varphi}_m(-39 - 9\bar{\varphi}_r^2 + 4\bar{\varphi}_r^3) + \bar{\varphi}_r(-1144 - 60\bar{\varphi}_r^2 + 15\bar{\varphi}_r^3)) + 2\delta^5(-1716 + 1320\bar{\varphi}_m^4 + 792\bar{\varphi}_r - 372\bar{\varphi}_r^2 + 62\bar{\varphi}_r^3 + 4\bar{\varphi}_r^4 - 60\bar{\varphi}_m^3(19 + 32\bar{\varphi}_r) + \\
 & 3\bar{\varphi}_m^2(-649 + 489\bar{\varphi}_r + 288\bar{\varphi}_r^2) - 2\bar{\varphi}_m(792 - 897\bar{\varphi}_r + 282\bar{\varphi}_r^2 + 64\bar{\varphi}_r^3)), a_9 = \delta(-4 + \delta(19 + 61\bar{\varphi}_m - 4\bar{\varphi}_m^2 - 9\bar{\varphi}_r) + \delta^2(355 + 101\bar{\varphi}_m^2 + 68\bar{\varphi}_r + \\
 & \bar{\varphi}_r^2 - \bar{\varphi}_m(235 + 44\bar{\varphi}_r)) - \delta^3(252\bar{\varphi}_m^3 - 8\bar{\varphi}_m^2(-94 + 27\bar{\varphi}_r) + 11(158 - 35\bar{\varphi}_r + 6\bar{\varphi}_r^2) + \bar{\varphi}_m(869 - 534\bar{\varphi}_r + 36\bar{\varphi}_r^2)) + \delta^4(1414 + 1792\bar{\varphi}_m^3 - \\
 & 2249\bar{\varphi}_r + 290\bar{\varphi}_r^2 - 32\bar{\varphi}_r^3 - 28\bar{\varphi}_m^2(-65 + 72\bar{\varphi}_r) + 2\bar{\varphi}_m(2249 - 800\bar{\varphi}_r + 288\bar{\varphi}_r^2) - 4\delta^5(-570 + 420\bar{\varphi}_m^4 + \bar{\varphi}_m^3(651 - 672\bar{\varphi}_r) - 875\bar{\varphi}_r - 48\bar{\varphi}_r^2 - \\
 & 28\bar{\varphi}_r^3 + 2\bar{\varphi}_r^4 + 7\bar{\varphi}_m^2(-29 - 123\bar{\varphi}_r + 48\bar{\varphi}_r^2) - 7\bar{\varphi}_m(-228 - 29\bar{\varphi}_r - 45\bar{\varphi}_r^2 + 8\bar{\varphi}_r^3) + 2\delta^7(3432\bar{\varphi}_m^4 + 594\bar{\varphi}_m^2\bar{\varphi}_r(-7 + 8\bar{\varphi}_r) - 858\bar{\varphi}_m^3(-3 + 8\bar{\varphi}_r) + \\
 & \bar{\varphi}_m(5005 + 2079\bar{\varphi}_r^2 - 1320\bar{\varphi}_r^3) + 3\bar{\varphi}_r(-1001 - 105\bar{\varphi}_r^2 + 40\bar{\varphi}_r^3)) + 2\delta^6(-1287 + 1848\bar{\varphi}_m^4 + 792\bar{\varphi}_r - 525\bar{\varphi}_r^2 + 126\bar{\varphi}_r^3 + 28\bar{\varphi}_r^4 - 42\bar{\varphi}_m^3(31 + \\
 & 80\bar{\varphi}_r) + 3\bar{\varphi}_m^2(-649 + 651\bar{\varphi}_r + 672\bar{\varphi}_r^2) - \bar{\varphi}_m(1419 - 2100\bar{\varphi}_r + 903\bar{\varphi}_r^2 + 448\bar{\varphi}_r^3)), a_{10} = -\delta(-4(3 + \bar{\varphi}_m) + \delta(36 - 16\bar{\varphi}_m^2 - 52\bar{\varphi}_r + 2\bar{\varphi}_m(69 + \\
 & 4\bar{\varphi}_r)) + \delta^2(355 + 195\bar{\varphi}_m^2 + 167\bar{\varphi}_r + 21\bar{\varphi}_r^2 - 2\bar{\varphi}_m(167 + 79\bar{\varphi}_r)) - \delta^3(1398 + 420\bar{\varphi}_m^3 + \bar{\varphi}_m^2(970 - 540\bar{\varphi}_r) - 484\bar{\varphi}_r + 201\bar{\varphi}_r^2 - 12\bar{\varphi}_r^3 + \bar{\varphi}_m(869 - \\
 & 970\bar{\varphi}_r + 180\bar{\varphi}_r^2) + \delta^4(864 + 2240\bar{\varphi}_m^3 - 2249\bar{\varphi}_r + 510\bar{\varphi}_r^2 - 160\bar{\varphi}_r^3 - 140\bar{\varphi}_m^2(-13 + 24\bar{\varphi}_r) + 6\bar{\varphi}_m(613 - 340\bar{\varphi}_r + 240\bar{\varphi}_r^2) + \delta^7(6006\bar{\varphi}_m^4 + \\
 & 792\bar{\varphi}_m^2\bar{\varphi}_r(-9 + 14\bar{\varphi}_r) - 429\bar{\varphi}_m^3(-9 + 32\bar{\varphi}_r) - 462\bar{\varphi}_m(-13 - 9\bar{\varphi}_r^2 + 8\bar{\varphi}_r^3) + 28\bar{\varphi}_r(-143 - 27\bar{\varphi}_r^2 + 15\bar{\varphi}_r^3) + \delta^5(1515 - 2016\bar{\varphi}_m^4 + 2884\bar{\varphi}_r + \\
 & 214\bar{\varphi}_r^2 + 308\bar{\varphi}_r^3 - 48\bar{\varphi}_r^4 + 84\bar{\varphi}_m^3(-31 + 48\bar{\varphi}_r) + \bar{\varphi}_m^2(730 + 4368\bar{\varphi}_r - 2688\bar{\varphi}_r^2) + 4\bar{\varphi}_m(-1119 - 203\bar{\varphi}_r - 546\bar{\varphi}_r^2 + 168\bar{\varphi}_r^3)) + 2\delta^6(-715 + \\
 & 1848\bar{\varphi}_m^4 + 627\bar{\varphi}_r - 525\bar{\varphi}_r^2 + 175\bar{\varphi}_r^3 + 84\bar{\varphi}_r^4 - 12\bar{\varphi}_m^3(95 + 336\bar{\varphi}_r) + 3\bar{\varphi}_m^2(-484 + 651\bar{\varphi}_r + 1008\bar{\varphi}_r^2) - 2\bar{\varphi}_m(506 - 897\bar{\varphi}_r + 525\bar{\varphi}_r^2 + 448\bar{\varphi}_r^3))), \\
 a_{11} = & \delta(4(-3 - 2\bar{\varphi}_m + \bar{\varphi}_r) + \delta(19 - 24\bar{\varphi}_m^2 - 86\bar{\varphi}_r - 4\bar{\varphi}_r^2 + 6\bar{\varphi}_m(23 + 4\bar{\varphi}_r)) + \delta^2(237 + 195\bar{\varphi}_m^2 + 167\bar{\varphi}_r + 58\bar{\varphi}_r^2 - \bar{\varphi}_m(235 + 232\bar{\varphi}_r)) + \\
 & \delta^4(284 + 1792\bar{\varphi}_m^3 - 1429\bar{\varphi}_r + 510\bar{\varphi}_r^2 - 320\bar{\varphi}_r^3 - 168\bar{\varphi}_m^2(-7 + 20\bar{\varphi}_r) + 20\bar{\varphi}_m(99 - 80\bar{\varphi}_r + 96\bar{\varphi}_r^2)) - \delta^3(708 + 420\bar{\varphi}_m^3 + \bar{\varphi}_m^2(752 - 720\bar{\varphi}_r) - \\
 & 385\bar{\varphi}_r + 284\bar{\varphi}_r^2 - 48\bar{\varphi}_r^3 + \bar{\varphi}_m(571 - 970\bar{\varphi}_r + 360\bar{\varphi}_r^2)) - 2\delta^5(-370 + 840\bar{\varphi}_m^4 + \bar{\varphi}_m^3(846 - 2016\bar{\varphi}_r) - 796\bar{\varphi}_r - 96\bar{\varphi}_r^2 - 210\bar{\varphi}_r^3 + 60\bar{\varphi}_r^4 + \\
 & 7\bar{\varphi}_m^2(-37 - 246\bar{\varphi}_r + 240\bar{\varphi}_r^2) + \bar{\varphi}_m(1077 + 324\bar{\varphi}_r + 1092\bar{\varphi}_r^2 - 560\bar{\varphi}_r^3) + \delta^7(4004\bar{\varphi}_m^4 - 429\bar{\varphi}_m^3(-5 + 24\bar{\varphi}_r) + 297\bar{\varphi}_m^2\bar{\varphi}_r(-15 + 32\bar{\varphi}_r) + \\
 & 14\bar{\varphi}_r(-143 - 45\bar{\varphi}_r^2 + 36\bar{\varphi}_r^3) - 6\bar{\varphi}_m(-455 - 495\bar{\varphi}_r^2 + 616\bar{\varphi}_r^3) + \delta^6(-572 + 2640\bar{\varphi}_m^4 + 770\bar{\varphi}_r - 744\bar{\varphi}_r^2 + 350\bar{\varphi}_r^3 + 280\bar{\varphi}_r^4 - 15\bar{\varphi}_m^3(101 + \\
 & 15\bar{\varphi}_r) + \bar{\varphi}_m^2(-1595 + 2934\bar{\varphi}_r + 6048\bar{\varphi}_r^2) - 2\bar{\varphi}_m(561 - 1110\bar{\varphi}_r + 903\bar{\varphi}_r^2 + 1120\bar{\varphi}_r^3)), a_{12} = -\delta(-4(1 + \bar{\varphi}_m - \bar{\varphi}_r) - \delta(2 + 16\bar{\varphi}_m^2 + 52\bar{\varphi}_r + \\
 & 8\bar{\varphi}_r^2 - \bar{\varphi}_m(61 + 24\bar{\varphi}_r)) + \delta^2(95 + 101\bar{\varphi}_m^2 + 68\bar{\varphi}_r + 58\bar{\varphi}_r^2 - 2\bar{\varphi}_m(37 + 79\bar{\varphi}_r)) - \delta^3(203 + 252\bar{\varphi}_m^3 + \bar{\varphi}_m^2(340 - 540\bar{\varphi}_r) - 186\bar{\varphi}_r + 201\bar{\varphi}_r^2 - 72\bar{\varphi}_r^3 + \\
 & \bar{\varphi}_m(233 - 534\bar{\varphi}_r + 360\bar{\varphi}_r^2)) + \delta^4(19 + 896\bar{\varphi}_m^3 - 551\bar{\varphi}_r + 290\bar{\varphi}_r^2 - 320\bar{\varphi}_r^3 - 8\bar{\varphi}_m^2(-59 + 252\bar{\varphi}_r) + \bar{\varphi}_m(665 - 752\bar{\varphi}_r + 1440\bar{\varphi}_r^2)) + \delta^7(2002\bar{\varphi}_m^4 + \\
 & 1980\bar{\varphi}_m^2\bar{\varphi}_r(-1 + 3\bar{\varphi}_r) - 286\bar{\varphi}_m^3(-3 + 20\bar{\varphi}_r) + \bar{\varphi}_m(910 + 1485\bar{\varphi}_r^2 - 2640\bar{\varphi}_r^3) + 4\bar{\varphi}_r(-182 - 90\bar{\varphi}_r^2 + 105\bar{\varphi}_r^3) + \delta^5(250 - 960\bar{\varphi}_m^4 + 562\bar{\varphi}_r + \\
 & 132\bar{\varphi}_r^2 + 308\bar{\varphi}_r^3 - 160\bar{\varphi}_r^4 + 6\bar{\varphi}_m^3(-113 + 448\bar{\varphi}_r) - 3\bar{\varphi}_m^2(-91 - 544\bar{\varphi}_r + 896\bar{\varphi}_r^2) + 4\bar{\varphi}_m(-169 - 97\bar{\varphi}_r - 315\bar{\varphi}_r^2 + 280\bar{\varphi}_r^3) + \delta^6(-156 + \\
 & 1320\bar{\varphi}_m^4 + 352\bar{\varphi}_r - 366\bar{\varphi}_r^2 + 252\bar{\varphi}_r^3 + 280\bar{\varphi}_r^4 - 20\bar{\varphi}_m^3(37 + 192\bar{\varphi}_r) + 3\bar{\varphi}_m^2(-209 + 537\bar{\varphi}_r + 1344\bar{\varphi}_r^2) - 2\bar{\varphi}_m(232 - 485\bar{\varphi}_r + 564\bar{\varphi}_r^2 + 896\bar{\varphi}_r^3))), \\
 a_{13} = & \delta^2(-3 - 4\bar{\varphi}_m^2 - 9\bar{\varphi}_r - 4\bar{\varphi}_r^2 + \bar{\varphi}_m(9 + 8\bar{\varphi}_r) + \delta(17 + 23\bar{\varphi}_m^2 + 6\bar{\varphi}_r + 21\bar{\varphi}_r^2 - \bar{\varphi}_m(5 + 44\bar{\varphi}_r)) - \delta^2(23 + 84\bar{\varphi}_m^3 + \bar{\varphi}_m^2(80 - 216\bar{\varphi}_r) - \\
 & 47\bar{\varphi}_r + 66\bar{\varphi}_r^2 - 48\bar{\varphi}_r^3 + \bar{\varphi}_m(51 - 146\bar{\varphi}_r + 180\bar{\varphi}_r^2)) + \delta^3(-17 + 256\bar{\varphi}_m^3 + \bar{\varphi}_m^2(106 - 672\bar{\varphi}_r) - 114\bar{\varphi}_r + 86\bar{\varphi}_r^2 - 160\bar{\varphi}_r^3 + 3\bar{\varphi}_m(41 - 64\bar{\varphi}_r + \\
 & 192\bar{\varphi}_r^2)) - 2\delta^4(-26 + 180\bar{\varphi}_m^4 + \bar{\varphi}_m^3(71 - 576\bar{\varphi}_r) - 57\bar{\varphi}_r - 31\bar{\varphi}_r^2 - 56\bar{\varphi}_r^3 + 60\bar{\varphi}_r^4 + \bar{\varphi}_m^2(-49 - 201\bar{\varphi}_r + 672\bar{\varphi}_r^2) + \bar{\varphi}_m(62 + 79\bar{\varphi}_r + 186\bar{\varphi}_r^2 - \\
 & 336\bar{\varphi}_r^3) + \delta^6(728\bar{\varphi}_m^4 + 66\bar{\varphi}_m^2\bar{\varphi}_r(-9 + 40\bar{\varphi}_r) - 26\bar{\varphi}_m^3(-9 + 88\bar{\varphi}_r) - 15\bar{\varphi}_m(-14 - 33\bar{\varphi}_r^2 + 88\bar{\varphi}_r^3) + \bar{\varphi}_r(-182 - 135\bar{\varphi}_r^2 + 240\bar{\varphi}_r^3) + \delta^5(-26 + \\
 & 440\bar{\varphi}_m^4 + 112\bar{\varphi}_r - 119\bar{\varphi}_r^2 + 124\bar{\varphi}_r^3 + 168\bar{\varphi}_r^4 - 10\bar{\varphi}_m^3(25 + 144\bar{\varphi}_r) + \bar{\varphi}_m^2(-167 + 609\bar{\varphi}_r + 1728\bar{\varphi}_r^2) - \bar{\varphi}_m(134 - 284\bar{\varphi}_r + 483\bar{\varphi}_r^2 + 896\bar{\varphi}_r^3))), \\
 a_{14} = & -\delta^3(\bar{\varphi}_m + \bar{\varphi}_m^2 - 2\bar{\varphi}_m\bar{\varphi}_r + (-1 + \bar{\varphi}_r)\bar{\varphi}_r + \delta(1 - 12\bar{\varphi}_m^3 + 4\bar{\varphi}_r - 7\bar{\varphi}_r^2 + 12\bar{\varphi}_r^3 + \bar{\varphi}_m^2(-7 + 36\bar{\varphi}_r) - 2\bar{\varphi}_m(2 - 7\bar{\varphi}_r + 18\bar{\varphi}_r^2)) + \delta^2(-4 + \\
 & 32\bar{\varphi}_m^3 + \bar{\varphi}_m^2(10 - 96\bar{\varphi}_r) - 9\bar{\varphi}_r + 10\bar{\varphi}_r^2 - 32\bar{\varphi}_r^3 + \bar{\varphi}_m(9 - 20\bar{\varphi}_r + 96\bar{\varphi}_r^2)) + \delta^5(182\bar{\varphi}_m^4 + \bar{\varphi}_m^3(39 - 624\bar{\varphi}_r) - 28\bar{\varphi}_r - 30\bar{\varphi}_r^3 + 90\bar{\varphi}_r^4 + \\
 & 36\bar{\varphi}_m^2\bar{\varphi}_r(-3 + 22\bar{\varphi}_r) + \bar{\varphi}_m(30 + 99\bar{\varphi}_r^2 - 440\bar{\varphi}_r^3) + \delta^3(5 - 80\bar{\varphi}_m^4 + 10\bar{\varphi}_r + 17\bar{\varphi}_r^2 + 12\bar{\varphi}_r^3 - 48\bar{\varphi}_r^4 + 6\bar{\varphi}_m^3(-1 + 48\bar{\varphi}_r) + \bar{\varphi}_m^2(21 + 24\bar{\varphi}_r -
 \end{aligned}$$

$$\begin{aligned}
 & 384\bar{\varphi}_r^2 + 2\bar{\varphi}_m(-5 - 19\bar{\varphi}_r - 15\bar{\varphi}_r^2 + 112\bar{\varphi}_r^3) + \bar{\delta}^4(-2 + 88\bar{\varphi}_m^4 + 22\bar{\varphi}_r - 23\bar{\varphi}_r^2 + 37\bar{\varphi}_r^3 + 56\bar{\varphi}_r^4 - 4\bar{\varphi}_m^3(13 + 80\bar{\varphi}_r) + 3\bar{\varphi}_m^2(-9 + 47\bar{\varphi}_r + 144\bar{\varphi}_r^2) - \\
 & 2\bar{\varphi}_m(12 - 25\bar{\varphi}_r + 63\bar{\varphi}_r^2 + 128\bar{\varphi}_r^3)), a_{15} = \bar{\delta}^6(\bar{\varphi}_m - \bar{\varphi}_r)(\bar{\delta}^2(2 + 28\bar{\varphi}_m^3 + \bar{\varphi}_m^2(3 - 76\bar{\varphi}_r) + 3\bar{\varphi}_r^2 - 20\bar{\varphi}_r^3 + 2\bar{\varphi}_m\bar{\varphi}_r(-3 + 34\bar{\varphi}_r)) + 2(-4\bar{\varphi}_m^3 + \\
 & \bar{\varphi}_m^2(1 + 12\bar{\varphi}_r) + \bar{\varphi}_m(1 - 2\bar{\varphi}_r - 12\bar{\varphi}_r^2) + \bar{\varphi}_r(-1 + \bar{\varphi}_r + 4\bar{\varphi}_r^2)) + \bar{\delta}(-2 + 8\bar{\varphi}_m^3 + 2\bar{\varphi}_r - 5\bar{\varphi}_r^2 - 8\bar{\varphi}_r^3 - \bar{\varphi}_m^2(5 + 24\bar{\varphi}_r) + 2\bar{\varphi}_m(-1 + 5\bar{\varphi}_r + 12\bar{\varphi}_r^2)), \\
 & a_{16} = -2\bar{\delta}^8(\bar{\varphi}_m - \bar{\varphi}_r)^4. \\
 & b_0 = -8\bar{\delta}^7\bar{\varphi}_m^3, b_1 = 8\bar{\delta}^6\bar{\varphi}_m^2(-2 + (-1 + 12\bar{\delta})\bar{\varphi}_m - 3\bar{\delta}\bar{\varphi}_r), b_2 = -8\bar{\delta}^5\bar{\varphi}_m(1 + \bar{\delta}(-7 + 66\bar{\delta})\bar{\varphi}_m^2 + 4\bar{\delta}\bar{\varphi}_r + 3\bar{\delta}^2\bar{\varphi}_r^2 + \bar{\varphi}_m(4 - 33\bar{\delta}^2\bar{\varphi}_r + \\
 & \bar{\delta}(-20 + 3\bar{\varphi}_r))), b_3 = 8\bar{\delta}^4(\bar{\delta}(-8 - 19\bar{\delta} + 220\bar{\delta}^2)\bar{\varphi}_m^3 - \bar{\delta}\bar{\varphi}_r(1 + \bar{\delta}\bar{\varphi}_r)^2 + \bar{\varphi}_m^2(-2 + 2\bar{\delta} + 18\bar{\delta}^2(-5 + \bar{\varphi}_r) - 165\bar{\delta}^3\bar{\varphi}_r) + \bar{\varphi}_m(-3 - 8\bar{\delta}(-1 + \\
 & \bar{\varphi}_r) - 3\bar{\delta}^2(-12 + \bar{\varphi}_r)\bar{\varphi}_r + 30\bar{\delta}^3\bar{\varphi}_r^2)), b_4 = -8\bar{\delta}^3(\bar{\delta}(4 - 64\bar{\delta} - 21\bar{\delta}^2 + 495\bar{\delta}^3)\bar{\varphi}_m^3 + \bar{\delta}\bar{\varphi}_r(3 + \bar{\delta}^2(-16 + \bar{\varphi}_r)\bar{\varphi}_r - 9\bar{\delta}^3\bar{\varphi}_r^2 + \bar{\delta}(-7 + 4\bar{\varphi}_r)) + \\
 & \bar{\varphi}_m(3 + \bar{\delta}^2(28 - 48\bar{\varphi}_r) + 135\bar{\delta}^4\bar{\varphi}_r^2 + \bar{\delta}(-17 + 4\bar{\varphi}_r) - 3\bar{\delta}^3\bar{\varphi}_r(-48 + 5\bar{\varphi}_r)) + \bar{\delta}\bar{\varphi}_m^2(8 - 495\bar{\delta}^3\bar{\varphi}_r + 8\bar{\delta}(11 + 3\bar{\varphi}_r) + 3\bar{\delta}^2(-80 + 13\bar{\varphi}_r))), \\
 & b_5 = 8\bar{\delta}^2(2\bar{\delta}^2(14 - 112\bar{\delta} + 3\bar{\delta}^2 + 396\bar{\delta}^3)\bar{\varphi}_m^3 - \bar{\delta}\bar{\varphi}_r(3 + \bar{\delta}^2(21 - 20\bar{\varphi}_r) + 2\bar{\delta}(-7 + \bar{\varphi}_r) - 4\bar{\delta}^3(-14 + \bar{\varphi}_r)\bar{\varphi}_r + 36\bar{\delta}^4\bar{\varphi}_r^2) - 2\bar{\delta}\bar{\varphi}_m^2(12 + 495\bar{\delta}^4\bar{\varphi}_r - \\
 & 84\bar{\delta}^2(1 + \bar{\varphi}_r) - 6\bar{\delta}^3(-35 + 2\bar{\varphi}_r) + \bar{\delta}(-44 + 6\bar{\varphi}_r)) + \bar{\varphi}_m(-1 + 2\bar{\delta} - 24\bar{\delta}^4(-14 + \bar{\varphi}_r)\bar{\varphi}_r + 360\bar{\delta}^5\bar{\varphi}_r^2 - \bar{\delta}^2(43 + 20\bar{\varphi}_r) - 8\bar{\delta}^3(-7 + 16\bar{\varphi}_r + 3\bar{\varphi}_r^2))), \\
 & b_6 = -8\bar{\delta}^2(14\bar{\delta}^2(6 - 32\bar{\delta} + 3\bar{\delta}^2 + 66\bar{\delta}^3)\bar{\varphi}_m^3 - 2\bar{\varphi}_m^2(-4 + 60\bar{\delta} + 693\bar{\delta}^5\bar{\varphi}_r + 21\bar{\delta}^4(12 + \bar{\varphi}_r) + 4\bar{\delta}^2(-31 + 9\bar{\varphi}_r) - 28\bar{\delta}^3(4 + 9\bar{\varphi}_r)) + \bar{\varphi}_r(1 + \\
 & \bar{\delta} + 4\bar{\delta}^4(-28 + \bar{\varphi}_r)\bar{\varphi}_r - 84\bar{\delta}^5\bar{\varphi}_r^2 + \bar{\delta}^2(29 + 12\bar{\varphi}_r) + \bar{\delta}^3(-35 + 44\bar{\varphi}_r + 8\bar{\varphi}_r^2)) + \bar{\varphi}_m(19 + 504\bar{\delta}^4\bar{\varphi}_r + 630\bar{\delta}^5\bar{\varphi}_r^2 + \bar{\delta}(-19 + 48\bar{\varphi}_r) + \bar{\delta}^2(-65 - \\
 & 156\bar{\varphi}_r + 12\bar{\varphi}_r^2) - 2\bar{\delta}^3(-35 + 104\bar{\varphi}_r + 72\bar{\varphi}_r^2)), b_7 = 8\bar{\delta}(2\bar{\delta}^3(70 - 280\bar{\delta} + 21\bar{\delta}^2 + 396\bar{\delta}^3)\bar{\varphi}_m^3 - 2\bar{\delta}\bar{\varphi}_m^2(-16 + 120\bar{\delta} + 693\bar{\delta}^5\bar{\varphi}_r + 42\bar{\delta}^4(5 + \bar{\varphi}_r) + \\
 & 10\bar{\delta}^2(-17 + 9\bar{\varphi}_r) - 28\bar{\delta}^3(4 + 15\bar{\varphi}_r)) - \bar{\delta}\bar{\varphi}_r(20 + 126\bar{\delta}^5\bar{\varphi}_r^2 + 4\bar{\delta}^4\bar{\varphi}_r(35 + \bar{\varphi}_r) + 6\bar{\delta}(-3 + 4\bar{\varphi}_r) + \bar{\delta}^2(-36 - 66\bar{\varphi}_r + 4\bar{\varphi}_r^2) - 5\bar{\delta}^3(-7 + 12\bar{\varphi}_r + \\
 & 8\bar{\varphi}_r^2)) + \bar{\varphi}_m(-16 + \bar{\delta}(6(2 - 16\bar{\varphi}_r) + 756\bar{\delta}^6\bar{\varphi}_r^2 + 42\bar{\delta}^5\bar{\varphi}_r(12 + \bar{\varphi}_r) + 12\bar{\delta}^2(-3 + 16\bar{\varphi}_r) + 5\bar{\delta}^3(-13 - 68\bar{\varphi}_r + 12\bar{\varphi}_r^2) - 8\bar{\delta}^4(-7 + 30\bar{\varphi}_r + 45\bar{\varphi}_r^2))), \\
 & b_8 = -8(\bar{\delta}^4(140 - 448\bar{\delta} + 6\bar{\delta}^2 + 495\bar{\delta}^3)\bar{\varphi}_m^3 - 2\bar{\delta}^2\bar{\varphi}_m^2(-24 + 120\bar{\delta} + 495\bar{\delta}^5\bar{\varphi}_r - 84\bar{\delta}^3(1 + 5\bar{\varphi}_r) + 3\bar{\delta}^4(40 + 7\bar{\varphi}_r) + 4\bar{\delta}^2(-31 + 30\bar{\varphi}_r)) + \\
 & \bar{\delta}\bar{\varphi}_r(16 + \bar{\delta}^2(18 - 72\bar{\varphi}_r) - 126\bar{\delta}^6\bar{\varphi}_r^2 - 2\bar{\delta}^5\bar{\varphi}_r(56 + 5\bar{\varphi}_r) + \bar{\delta}(-42 + 8\bar{\varphi}_r) + \bar{\delta}^3(29 + 104\bar{\varphi}_r - 16\bar{\varphi}_r^2) + \bar{\delta}^4(-21 + 60\bar{\varphi}_r + 80\bar{\varphi}_r^2)) + \bar{\varphi}_m(4 - \\
 & 32\bar{\delta} + \bar{\delta}^2(62 - 48\bar{\varphi}_r) + 630\bar{\delta}^7\bar{\varphi}_r^2 + 42\bar{\delta}^6\bar{\varphi}_r(8 + \bar{\varphi}_r) + \bar{\delta}^3(-19 + 288\bar{\varphi}_r) + \bar{\delta}^4(-43 - 340\bar{\varphi}_r + 120\bar{\varphi}_r^2) - 4\bar{\delta}^5(-7 + 52\bar{\varphi}_r + 120\bar{\varphi}_r^2))), \\
 & b_9 = 8(\bar{\delta}^4(84 - 224\bar{\delta} - 21\bar{\delta}^2 + 220\bar{\delta}^3)\bar{\varphi}_m^3 + \bar{\delta}^2\bar{\varphi}_m^2(32 - 120\bar{\delta} + \bar{\delta}^2(88 - 180\bar{\varphi}_r) - 495\bar{\delta}^5\bar{\varphi}_r + 6\bar{\delta}^4(-15 + 4\bar{\varphi}_r) + 8\bar{\delta}^3(11 + 63\bar{\varphi}_r)) + \\
 & \bar{\varphi}_r(-4 + 16\bar{\delta} + \bar{\delta}^3(1 - 72\bar{\varphi}_r) - 84\bar{\delta}^7\bar{\varphi}_r^2 - 4\bar{\delta}^6\bar{\varphi}_r(14 + \bar{\varphi}_r) + 4\bar{\delta}^2(-5 + 4\bar{\varphi}_r) + \bar{\delta}^4(14 + 66\bar{\varphi}_r - 24\bar{\varphi}_r^2) + \bar{\delta}^5(-7 + 44\bar{\varphi}_r + 80\bar{\varphi}_r^2)) + \\
 & \bar{\varphi}_m(4 - 16\bar{\delta} + \bar{\delta}^2(19 - 48\bar{\varphi}_r) + 144\bar{\delta}^6\bar{\varphi}_r + 360\bar{\delta}^7\bar{\varphi}_r^2 + 2\bar{\delta}^3(1 + 96\bar{\varphi}_r) - 8\bar{\delta}^5(-1 + 16\bar{\varphi}_r + 45\bar{\varphi}_r^2) + \bar{\delta}^4(-17 - 156\bar{\varphi}_r + 120\bar{\varphi}_r^2))), \\
 & b_{10} = 8\bar{\delta}^2((-4 + 8\bar{\delta} - 5\bar{\delta}^3)(2 - 2\bar{\delta} + \bar{\delta}^2(7\bar{\varphi}_m - 4\bar{\varphi}_r))(\bar{\varphi}_m - \bar{\varphi}_r)^2 - 2\bar{\delta}^3(-4 + \bar{\delta} + 5\bar{\delta}^2)(\bar{\varphi}_m - \bar{\varphi}_r)^3 - (-1 + \bar{\delta})(21\bar{\delta}^4\bar{\varphi}_m^3 + \bar{\delta}^2\bar{\varphi}_m^2(8 - \\
 & 10\bar{\delta} - 45\bar{\delta}^2\bar{\varphi}_r) - \bar{\varphi}_r(1 - 2\bar{\delta} + \bar{\delta}^2(1 - 4\bar{\varphi}_r) + 6\bar{\delta}^3\bar{\varphi}_r + 6\bar{\delta}^4\bar{\varphi}_r^2) + \bar{\varphi}_m(1 - 2\bar{\delta} + \bar{\delta}^2(1 - 12\bar{\varphi}_r) + 16\bar{\delta}^3\bar{\varphi}_r + 30\bar{\delta}^4\bar{\varphi}_r^2)), b_{11} = 8\bar{\delta}^4(\bar{\varphi}_m - \\
 & \bar{\varphi}_r)^2(-2 + 4\bar{\varphi}_m + 3\bar{\delta}^3(4\bar{\varphi}_m - 3\bar{\varphi}_r) - 4\bar{\varphi}_r + \bar{\delta}^2(-2 - 7\bar{\varphi}_m + 4\bar{\varphi}_r) + \bar{\delta}(4 - 8\bar{\varphi}_m + 8\bar{\varphi}_r)), b_{12} = -8(-1 + \bar{\delta})\bar{\delta}^6(\bar{\varphi}_m - \bar{\varphi}_r)^3.
 \end{aligned}$$

C Simulation procedures

Procedure 1 Iterate system (4) until it converges

Input: Default parameter set ψ and initial state of variables

Output: Stability range l_x and its length $|l_x|$

procedure

Find $\alpha_{min}, \alpha_{max} \in (0, 1)$ such that $P(\alpha_i) = 0$ with $i \in \{min, max\}$;

Define $X(s) = (u(s), v(s), w(s))$;

for $\alpha \in (\alpha_{min}, \alpha_{max})$ **do**

Simulate system (4) on interval $[0, T]$ for T large enough or until $|u_n - u^*(\alpha)| < \epsilon_0$ and $|\bar{u}_k - \underline{u}_k| < \epsilon_0$ where $u_k = median\{u(s) : s_k < s < s_{k+1}\}$, $\bar{u}_k = \max\{u(s) : s_k < s < s_{k+1}\}$ and $\underline{u}_k = \min\{u(s) : s_k < s < s_{k+1}\}$ for a designate positive tolerance ϵ ;

if $|u_k - u^*(\alpha)| < \epsilon_0$ and $|\bar{u}_k - \underline{u}_k| < \epsilon_0$ **then**

$\alpha \in l_x$;

end if

end for

if $l_x \neq \emptyset$ **then**

Calculate $|l_x| = \max\{l_x\} - \min\{l_x\}$;

else

$|l_x| = 0$;

end if

end procedure

Procedure 2 Iterate system (7) for stability/instability behaviors finds

Input: Default parameter set ξ and initial state of variables

Output: Classification matrix \mathcal{M} of temporal dynamics of model (7): $\mathcal{M}_{i,j} = 1$ (Stable trajectory a fixed value), $\mathcal{M}_{i,j} = 0.66$ (Periodic trajectory), $\mathcal{M}_{i,j} = 0.33$ (Quasi-periodic trajectory), and $\mathcal{M}_{i,j} = 0$ (Unrestricted trajectory)

procedure

Define $X(s) = (\alpha(s), u(s), v(s), w(s))$;

for $(x, y) \in \{(U_0, \sigma_0), (\sigma_0, \theta), (\theta, U_0), (\tau, l), (U_0, c)\}$ such that $(x, y) \in I \times J \subset \mathbb{R}_+^2$ where $I = \{x_1, \dots, x_{m_1}\}$ and $J = \{y_1, \dots, y_{m_2}\}$ **do**

 Simulate system (7) on interval $[0, T]$ for T large enough or until obtain

- (i) $\alpha(\tau_k) > \delta_0$ and $|\bar{u}_k - u^*(\alpha(\tau_k))| < \epsilon_0$ and $|G(z(\tau_k))| < \delta_1$ where $\bar{u}_k = \text{median}\{u(s) : s_k < s < s_{k+1}\}$, or
- (ii) $u(\tau_k) = \infty$ or $\alpha(\tau_k) \leq \delta_0$, for $T \geq \tau_k$ and designate positive tolerances $\epsilon, \delta_0, \delta_1$ and δ_2 ;

 Define $\bar{\tau}_k = \min\{\tau_k, T\}$, $D_1 = \{d_n = |\bar{u}_n - u^*(\alpha(\bar{\tau}_k))| : [0.98k] \leq n \leq k\}$, $D_2 = \{n : \Delta d_n > 0\}$, and $\mathcal{M} = \mathbf{0}_{m_2 \times m_1}$;

if $\alpha(\bar{\tau}_k) > \delta_0$ and $|\bar{u}_k - u^*(\alpha(\bar{\tau}_k))| < \epsilon_0$ and $|\Delta\alpha(\bar{\tau}_k)| < \delta_1$ **then**

$\mathcal{M}_{i,j} = 1$;

else

if $\alpha(\bar{\tau}_k) > \delta_0$ and $\#D_1 \neq \#D_2 + 1$ **then**

if $|G(z(\bar{\tau}_k))| \geq \delta_1$ and $|\Delta(|G(z(\bar{\tau}_k))|)| < \delta_2$ **then**

$\mathcal{M}_{i,j} = 0.66$;

else

if $|G(z(\bar{\tau}_k))| < \delta_1$ **then**

$\mathcal{M}_{i,j} = 1$;

else

$\mathcal{M}_{i,j} = 0.33$;

end if

end if

end if

end for

end procedure

Procedure 3 Iterate system (7) until it converges

Input: Default parameter set ξ and initial state of variables

Output: Extension of stability range \mathcal{L}_x

procedure

Define $X(s) = (\alpha(s), u(s), v(s), w(s))$;

for $\alpha_0 \in [0, 1]$ **do**

 Simulate system (7) on interval $[0, T]$ for T large enough or until $\alpha(\tau_k) > \delta_0$ and $|u_k - u^*(\alpha(\tau_k))| < \epsilon_0$ and $|\bar{u}_k - \underline{u}_k| < \epsilon_0$ and $|G(z(\tau_k))| < \delta_1$ where $u_k = \text{median}\{u(s) : s_k < s < s_{k+1}\}$, $\bar{u}_k = \max\{u(s) : s_k < s < s_{k+1}\}$ and $\underline{u}_k = \min\{u(s) : s_k < s < s_{k+1}\}$ for designated positive tolerances ϵ, δ_0 , and δ_1 ;

 Define $\bar{\tau}_k = \min\{\tau_k, T\}$;

if $\alpha(\bar{\tau}_k) > \delta_0$ and $|u_k - u^*(\alpha(\bar{\tau}_k))| < \epsilon_0$ and $|\bar{u}_k - \underline{u}_k| < \epsilon_0$ and $|G(z(\bar{\tau}_k))| < \delta_1$ **then**

$\alpha_0 \in \mathcal{L}_x$;

end if

end for

end procedure

References

- Agrawal AA (2001) Phenotypic plasticity in the interactions and evolution of species. *Science* 294(5541):321–326
- Akhmetzhanov AR, Grognard F, Mailleret L (2011) Optimal life history strategies in seasonal consumer-resource dynamics. *Evolution* 65:113–3125
- Alonso SH, Kindsvater HK (2008) Life-history patterns. In: Jørgensen SE, Fath BD (eds) *Encyclopedia of Ecology*. Academic Press, Oxford, pp 2929–2940
- Arditi R, Berryman AA (1991) The biological control paradox. *Trends Ecol Evol* 6:32
- Arditi R, Ginzburg LR (1989) Coupling in predator-prey dynamics: ratio-dependence. *J Theor Biol* 139:311–326
- Ashander J, Chevin L-M, Baskett ML (2016) Predicting evolutionary rescue via evolving plasticity in stochastic environments. *Proc R Soc B: Biol Sci* 283(1839):20161690
- Auld JR, Agrawal AA, Relyea RA (2010) Re-evaluating the costs and limits of adaptive phenotypic plasticity. *Proc Biol Sci* 277:503–511
- Bellard C, Bertelsmeier C, Leadley P, Thuiller W, Courchamp F (2012) Impacts of climate change on the future of biodiversity. *Ecol Lett* 15:365–377
- Berryman A (1992) The origins and evolution of predator-prey theory. *Ecology* 73:1530–1534
- Blueweiss L, Fox H, Kudzma V, Nakashima D, Peters R, Sams S (1978) Relationships between body size and some life history parameters. *Oecologia* 37:257–273
- Boggs C (1992) Resource allocation: exploring connections between foraging and life history. *Funct Ecol* 6:508–518
- Bonamour S, Chevin L-M, Charmantier A, Teplitsky C (2019) Phenotypic plasticity in response to climate change: the importance of cue variation. *Phil Trans R Soc B* 374:20180178
- Chevin L-M, Hoffmann AA (2017) Evolution of phenotypic plasticity in extreme environments. *Philos Trans R Soc B: Biol Sci* 372:20160138
- Chevin L-M, Lande R (2010) When do adaptive plasticity and genetic evolution prevent extinction of a density-regulated population? *Evolution* 64(4):1143–1150
- Chevin L-M, Lande R (2015) Evolution of environmental cues for phenotypic plasticity. *Evolution* 69(10):2767–2775
- Chevin L-M, Lande R, Mace GM (2010) Adaptation, plasticity, and extinction in a changing environment: towards a predictive theory. *PLoS Biol* 8:e1000357
- Chevin L-M, Romain G, Gomulkiewicz R, Holt R, Fellous S (2013) Phenotypic plasticity in evolutionary rescue experiments. *Philos Trans R Soc B: Biol Sci* 368(1610):20120089–20120089
- de Roos AM, Schellekens T, Van Kooten T, Van De Wolfshaar K, Claessen D, Persson L (2008) Simplifying a physiologically structured population model to a stage-structured biomass model. *Theor Popul Biol* 73:47–62
- DeLong JP, Hanley TC, Vasseur DA (2014) Predator-prey dynamics and the plasticity of predator body size. *Funct Ecol* 28(2):487–493
- DeWitt TJ, Sih A, Wilson DS (1998) Costs and limits of phenotypic plasticity. *Trends Ecol Evol* 13(2):77–81
- Ellers J, van Alphen JJM (1997) Life history evolution in *Asobara tabida*: plasticity in allocation of fat reserves to survival and reproduction. *J Evol Biol* 10:771–785
- Engen S, Saether BE (1994) Optimal allocation of resources to growth and reproduction. *Theor Popul Biol* 46:232–248
- Fischer B, Taborsky B, Dieckmann U (2009) Unexpected patterns of plastic energy allocation in stochastic environments. *Am Nat* 173:108–120
- Fischer B, Dieckmann U, Taborsky B (2010) When to store energy in a stochastic environment. *Evolution* 65:1221–1232
- Fox RJ, Donelson JM, Schunter C, Ravasi T, Gaitán-Espitia JD (2019) Beyond buying time: the role of plasticity in phenotypic adaptation to rapid environmental change. *Philos Trans R Soc B: Biol Sci* 374:20180174
- Getz WM (1984) Population dynamics: a per capita resource approach. *J Theor Biol* 108:623–643
- Getz WM (2009) Population and evolutionary dynamics of consumer-resource systems. In: McGlade J (ed) *Adv Ecol Theory: Princ Appl*. Wiley-Blackwell, Oxford, pp 194–231
- Getz WM (2011) Biomass transformation webs provide a unified approach to consumer-resource modelling. *Ecol Lett* 14(2):113–124

- Getz WM (2012) A biomass flow approach to population models and food webs. *Nat Resour Model* 25(1):93–121
- Ghalambor CK, McKay JK, Carroll SP, Reznick DN (2007) Adaptive versus non-adaptive phenotypic plasticity and the potential for contemporary adaptation in new environments. *Funct Ecol* 21(3):394–407
- Giuseppe F, Minelli A (2010) Phenotypic plasticity in development and evolution: facts and concepts. *Proc R Soc B: Biol Sci* 365(1540):547–556
- González-Olivares E, Rojas-Palma A (2013) Allee effect in Gause type predator-prey models: existence of multiple attractors, limit cycles and separatrix curves. a brief review. *Math Model Nat Phenom* 8:143–164
- González-Olivares E, Mena-Lorca J, Rojas-Palma A, Flores JD (2011) Dynamical complexities in the Leslie-Gower predator-prey model as consequences of the Allee effect on prey. *Appl Math Model* 35:366–381
- González-Olivares E, Meneses-Alcay H, González-Yañez B, Mena-Lorca J, Rojas-Palma A, Ramos-Jiliberto R (2011) Multiple stability and uniqueness of the limit cycle in a Gause-type predator-prey model considering the Allee effect on prey. *Nonlinear Anal Real World Appl* 12:2931–2942
- Gutiérrez R, Córdova-Lepe F, Moreno-Gómez FN, Velásquez NA (2020) Persistence and size of seasonal populations on a consumer-resource relationship depends on the allocation strategy toward life-history functions. *Sci Rep* 10:21401
- Heino M, Kaitala V (1999) Evolution of resource allocation between growth and reproduction in animals with indeterminate growth. *J Evol Biol* 12:423–429
- Hendry AP (2015) Key questions on the role of phenotypic plasticity in eco-evolutionary dynamics. *J Hered* 107(1):25–41
- Hoffmann AA, Sgrò CM (2011) Climate change and evolutionary adaptation. *Nature* 470:479–485
- Johansson J, Brannstrom A, Metz JAJ, Dieckmann U (2018) Twelve fundamental life histories evolving through allocation-dependent fecundity and survival. *Ecol Evol* 8(6):3172–3186
- Keyfitz N, Caswell H (2005) *Applied Mathematical Demography*, 3rd edn. Springer-Verlag, New York
- Kooijman SALM (2000) *Dynamic Energy and Mass Budgets in Biological Systems*, 2nd edn. Cambridge University Press, Cambridge
- Kovach-Orr C, Fussmann GF (2012) Evolutionary and plastic rescue in multitrophic model communities. *Philos Trans R Soc B: Biol Sci* 368(1610):20120084–20120084
- Kozłowski J, Wiegert RG (1986) Optimal allocation of energy to growth and reproduction. *Theor Popul Biol* 29:16–37
- Lakshmikantham V, Bainov D, Simeonov P (1989) *Theory of Impulsive Differential Equation*. World Scientific, NJ
- Mailleret L, Lemesle V (2009) A note on semi-discrete modelling in the life sciences. *Philos Trans R Soc A: Math Phys Eng Sci* 367:4779–4799
- Miner BG, Sultan SE, Morgan SG, Padilla DK, Relyea RA (2005) Ecological consequences of phenotypic plasticity. *Trends Ecol Evol* 20(12):685–692
- Murren C, Auld J, Callahan H, Ghalambor K, Handelsman C, Heskell M, Kingsolver J, Maclean H, Masel J, Maughan H, Pfennig D, Relyea R, Seiter S, Snell-Rood E, Steiner U, Schlichting C (2015) Constraints on the evolution of phenotypic plasticity: limits and costs of phenotype and plasticity. *Heredity* 115:293–301
- Ng'oma E, Perinchery AM, King EG (2017) How to get the most bang for your buck: the evolution and physiology of nutrition-dependent resource allocation strategies. *Proc R Soc B: Biol Sci* 284(1857):20170445
- Nijhout H (2003) Development and evolution of adaptive polyphenisms. *Evol Dev* 5(1):9–18
- Peñuelas J, Sardans J, Estiarte M, Ogaya R, Carnicer J, Coll M, Jump AS (2013) Evidence of current impact of climate change on life: a walk from genes to the biosphere. *Ecol Lett* 19:2303–2338
- Perrin N, Sibly R (1993) Dynamic models of energy allocation and investment. *Annu Rev Ecol Syst* 24:379–410
- Pigliucci M (2005) Evolution of phenotypic plasticity: where are we going now? *Trends Ecol Evol* 20(9):481–486
- Ramos-Jiliberto R (2005) Resource-consumer models and the biomass conversion principle. *Environ Model Softw* 20:85–91
- Reed TE, Waples RS, Schindle DE, Hard JJ, Kinnison MT (2010) Phenotypic plasticity and population viability: the importance of environmental predictability. *Proc R Soc B: Biol Sci* 277(1699):3391–3400

- Rosenzweig ML (1971) Paradox of enrichment: destabilization of exploitation ecosystems in ecological time. *Science* 171:385–387
- Samoilenko AM, Perestyuk NA (1995) Impulsive differential equations. World scientific series on nonlinear science. Series a: monographs and treatises, vol 14, World Scientific, Singapore
- Schlaepfer MA, Runge MC, Sherman PW (2002) Ecological and evolutionary traps. *Trends Ecol Evol* 17(10):474–480
- Soudijn FH, de Roos AM (2016) Approximation of a physiologically structured population model with seasonal reproduction by a stage-structured biomass model. *Thyroid Res* 10:73–90
- Staňková K, Abate A, Sabelis MW (2012) Irreversible prey diapause as an optimal strategy of a physiologically extended Lotka–Volterra model. *J Math Biol* 66:767–794
- Stankova K, Abate A, Sabelis MW, Busa J, You L (2013) Joining or opting out of a Lotka–Volterra game between predators and prey: does the best strategy depend on modelling energy lost and gained? *Interface Focus* 3:20130034–20130034
- Staňková K, Abate A, Sabelis MW (2013) Intra-seasonal strategies based on energy budgets in a dynamic predator–prey game. In: Vlastimil Křivan GZ (ed) *Advances in Dynamic Games: Theory, Applications, and Numerical Methods*. Birkhäuser, Basel, pp 205–221
- Steiner UK, Tuljapurkar S, Coulson T (2014) Generation time, net reproductive rate, and growth in stage-age-structured populations. *Am Nat* 183(6):771–783
- Stelzer CP (2001) Resource limitation and reproductive effort in a planktonic rotifer. *Ecology* 82:2521–2533
- Sun Z, de Roos AM (2015) Alternative stable states in a stage-structured consumer–resource biomass model with niche shift and seasonal reproduction. *Theor Popul Biol* 103:60–70
- Sun Z, de Roos AM (2017) Seasonal reproduction leads to population collapse and an Allee effect in a stage-structured consumer–resource biomass model when mortality rate increases. *PLoS ONE* 12:e0187338
- Sun Z, Parvinen K, Heino M, Metz JAJ, de Roos AM, Dieckmann U (2020) Evolution of reproduction periods in seasonal environments. *Am Nat* 196(4):E88–E109
- Takimoto G (2003) Adaptive plasticity in ontogenetic niche shifts stabilizes consumer–resource dynamics. *Am Nat* 162:93–109
- Thiel T, Gaschler S, Mody K, Blüthgen N, Drossel B (2021) Impact of herbivore preference on the benefit of plant trait variability. *Thyroid Res* 14:173–187
- Van Buskirk J, Steiner U (2009) The fitness costs of developmental canalization and plasticity. *J Evol Biol* 22(4):852–860
- Van Kleunen M, Fischer M (2005) Constraints on the evolution of adaptive phenotypic plasticity in plants. *New Phytol* 166(1):49–60
- Van Noordwijk AJ, de Jong G (1986) Acquisition and allocation of resources: their influence on variation in life history tactics. *Am Nat* 128(1):137–142
- West-Eberhard MJ (2008) Phenotypic plasticity. In: Jørgensen SE, Fath BD (eds) *Encyclopedia of Ecology*. Academic Press, Oxford, pp 2701–2707
- Wong BBM, Candolin U (2014) Behavioral responses to changing environments. *Behav Ecol* 26:665–673
- Ziółko M, Kozłowski J (1983) Evolution of body size: an optimization model. *Math Biosci* 64:127–143

Publisher's Note Springer Nature remains neutral with regard to jurisdictional claims in published maps and institutional affiliations.

Springer Nature or its licensor (e.g. a society or other partner) holds exclusive rights to this article under a publishing agreement with the author(s) or other rightsholder(s); author self-archiving of the accepted manuscript version of this article is solely governed by the terms of such publishing agreement and applicable law.